Snow Cover Fraction and Frozen Soil Distribution Simulated by CLM3 and Some Updated Schemes

Weiping Li, Kun Xia, Yong Luo

National Climate Center, CMA

liwp@cma.gov.cn

June 21, 2011, Breckenridge, Colorado

16th Annual CESM Workshop

Outline

Part I: Snow Cover Fraction

1. Background
2. Data, Experiments
3. Results
4. Summary and Discussion

1. Background

Snow Cover Fraction (SCF)

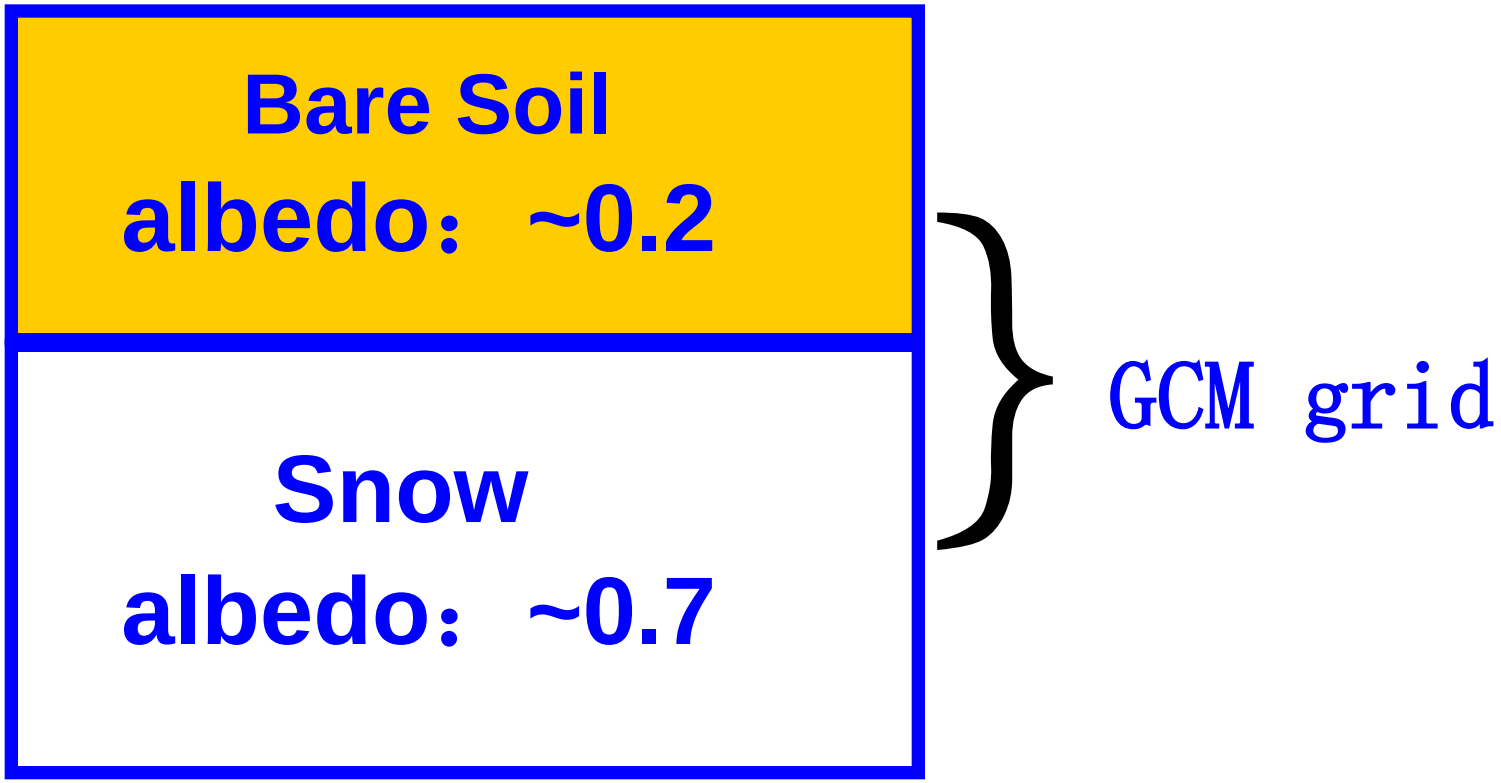

SCF: % of a GCM grid covered by snow

Uncertainties of SCF exist in climate models

SCF Schemes（Snow depth、SWE）

CLM3 (BATS) $f_{sno} = \dfrac{h_{sno}}{10 z_{0g} + h_{sno}}$

Wu2004 $f_{sno} = \min(1, \dfrac{a \cdot h_{sno}}{10.6 + h_{sno}})$

Yang1997 $f_{sno} = \tanh(\dfrac{h_{sno}}{2.5 z_{0,g}})$

Niu2007 $f_{sno} = \tanh(\dfrac{h_{sno}}{2.5 z_{0g} (\rho_{sno} / \rho_{new})^m})$

Douville1995 $f_{sno} = \dfrac{s_n}{s_n + 10} \cdot \sqrt{\dfrac{s_n}{s_n + \max(1.0, 0.15\sigma_z)}}$

Roesch2001 $f_{sno} = 0.95 \tanh(0.1 \cdot s_n) \sqrt{\dfrac{s_n}{s_n + \varepsilon + 0.15\sigma_z}}$

(From Niu and Yang, 2007)

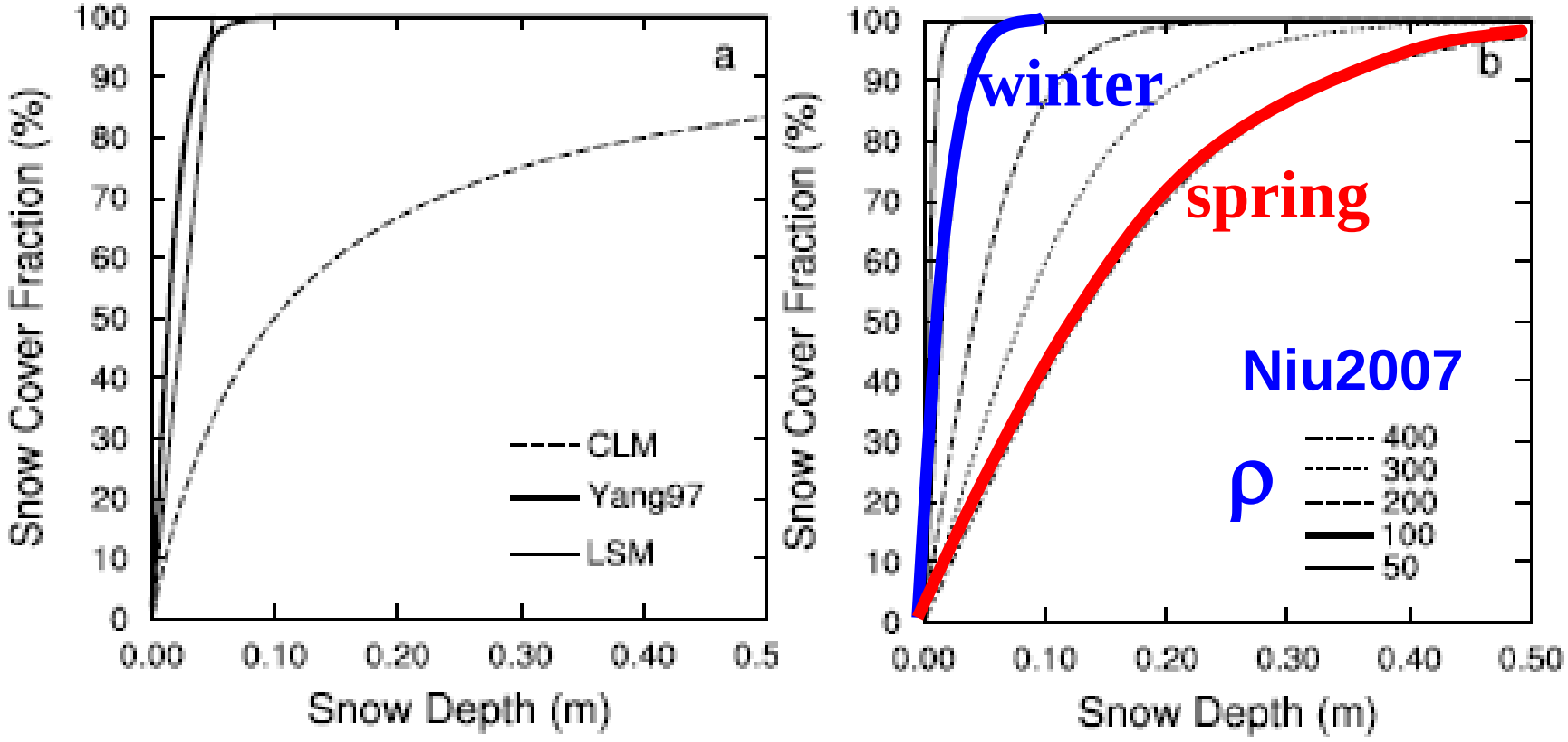

Snow density $\rho \geq \rho_{new}$

Niu2007 < Yang1997

Validation of different SCF schemes

2. Data, Experiment design

- **SCF observation:**

  NOAA AVHRR (1980-1995)

  MODIS (2001-2008)

- **Forcing: Qian (2006, NCEP) (1980-95)**

  GLDAS (2001-2008)

- **Exp：offline run of NCAR CLM3 (T42)**

  with different SCF schemes

  16-year (8-year) monthly mean

seasonal evolution of AVHRR SCF

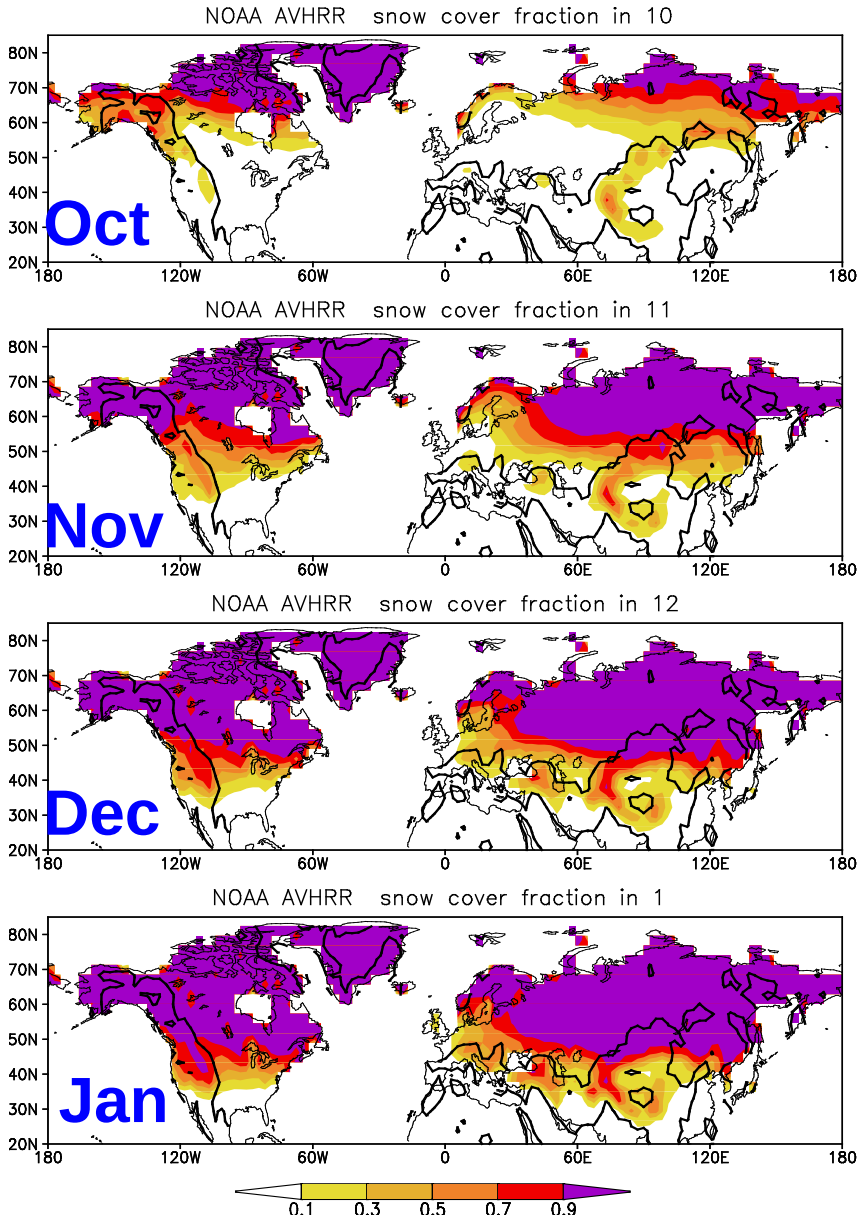

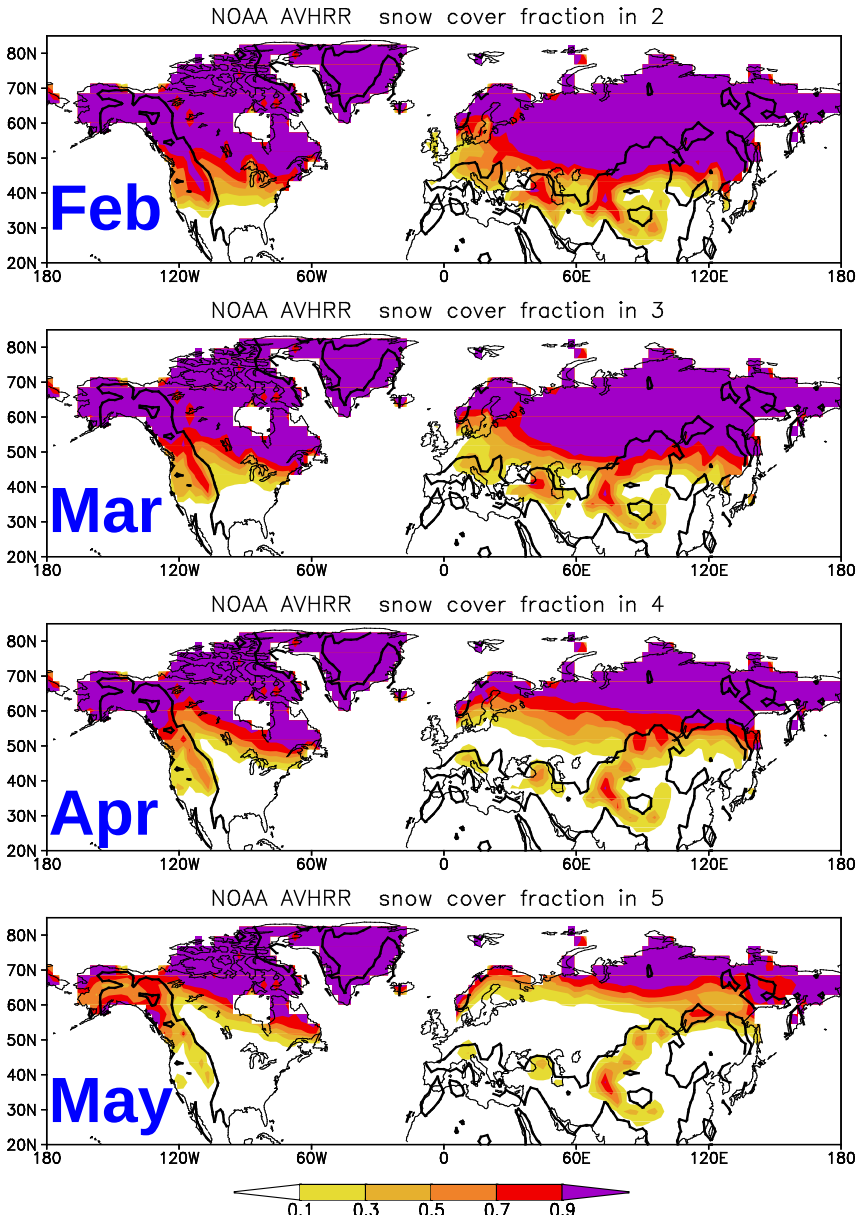

Simulated SCF – AVHRR SCF in February

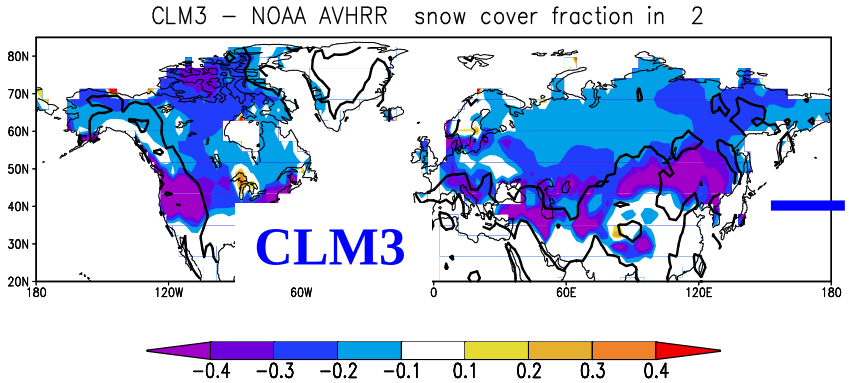

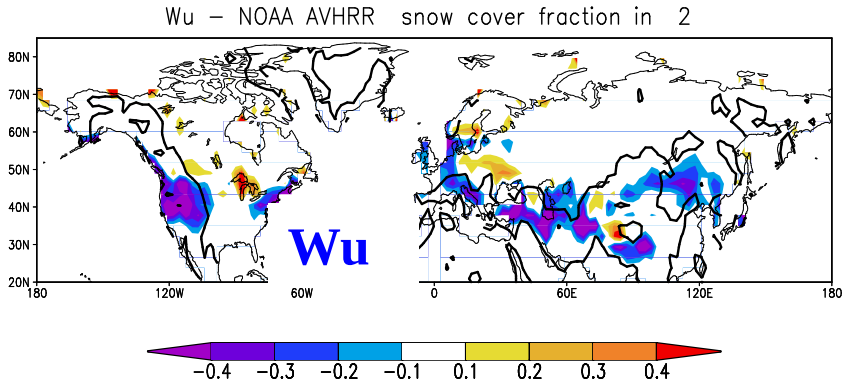

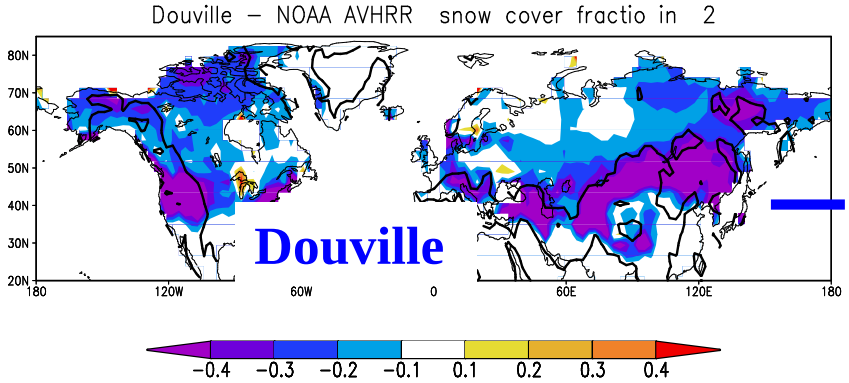

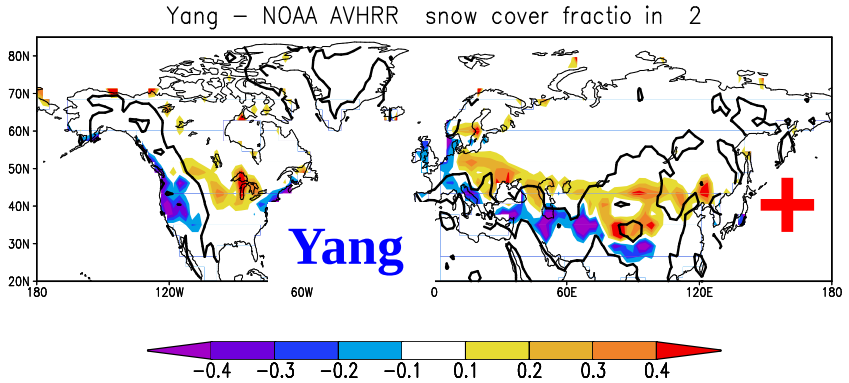

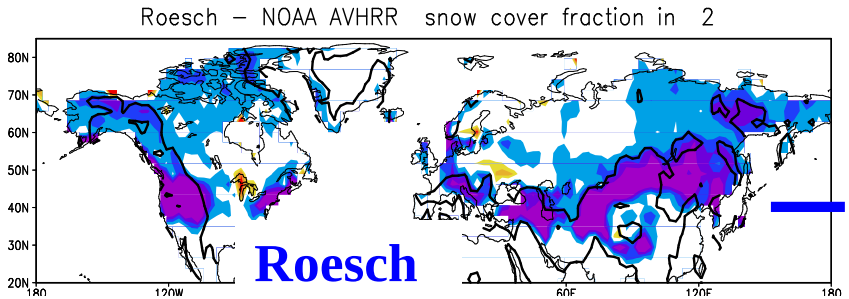

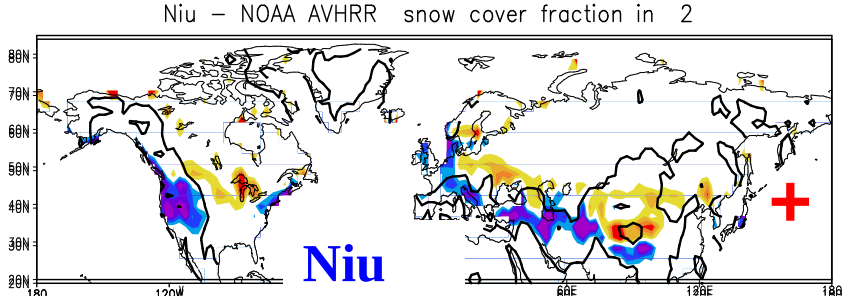

Seasonal evolution of areal mean SCF Simulations – AVHRR

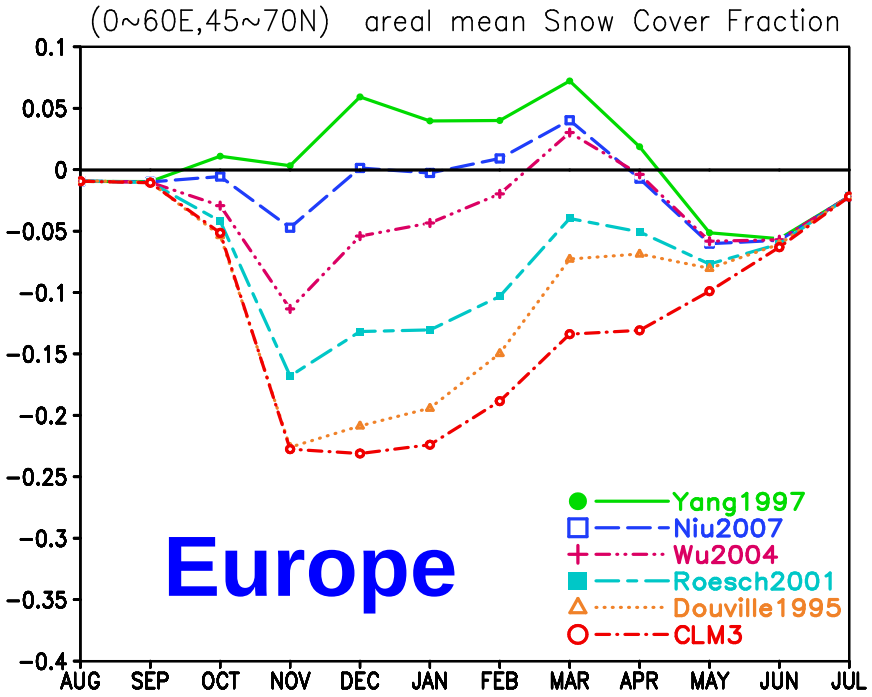

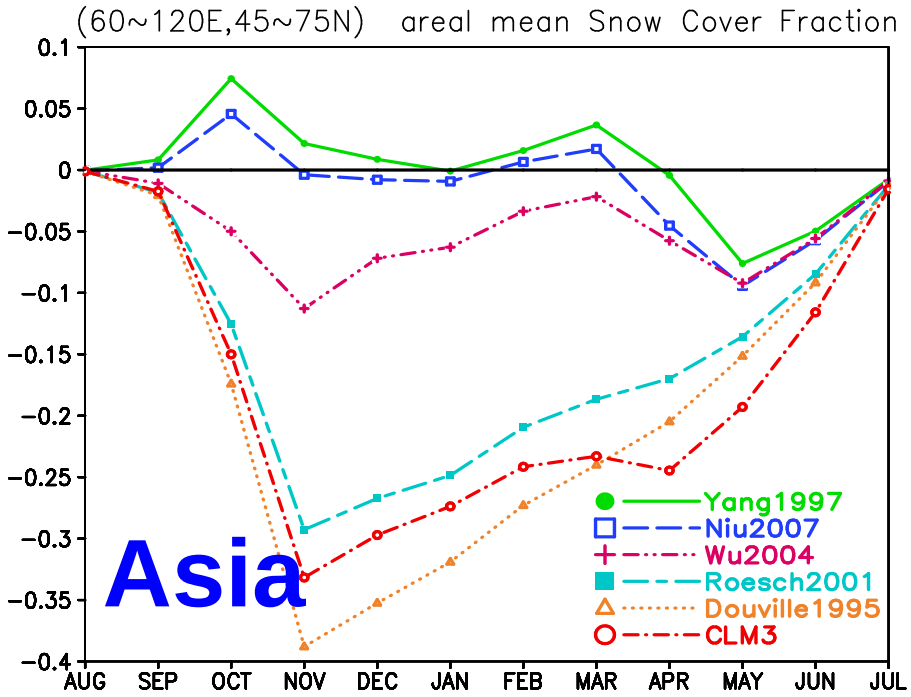

CLM3、Douville1995、Roesch2001: (–)

Yang1997: (+); Niu2007: (√)

Simulations – AVHRR areal mean SCF

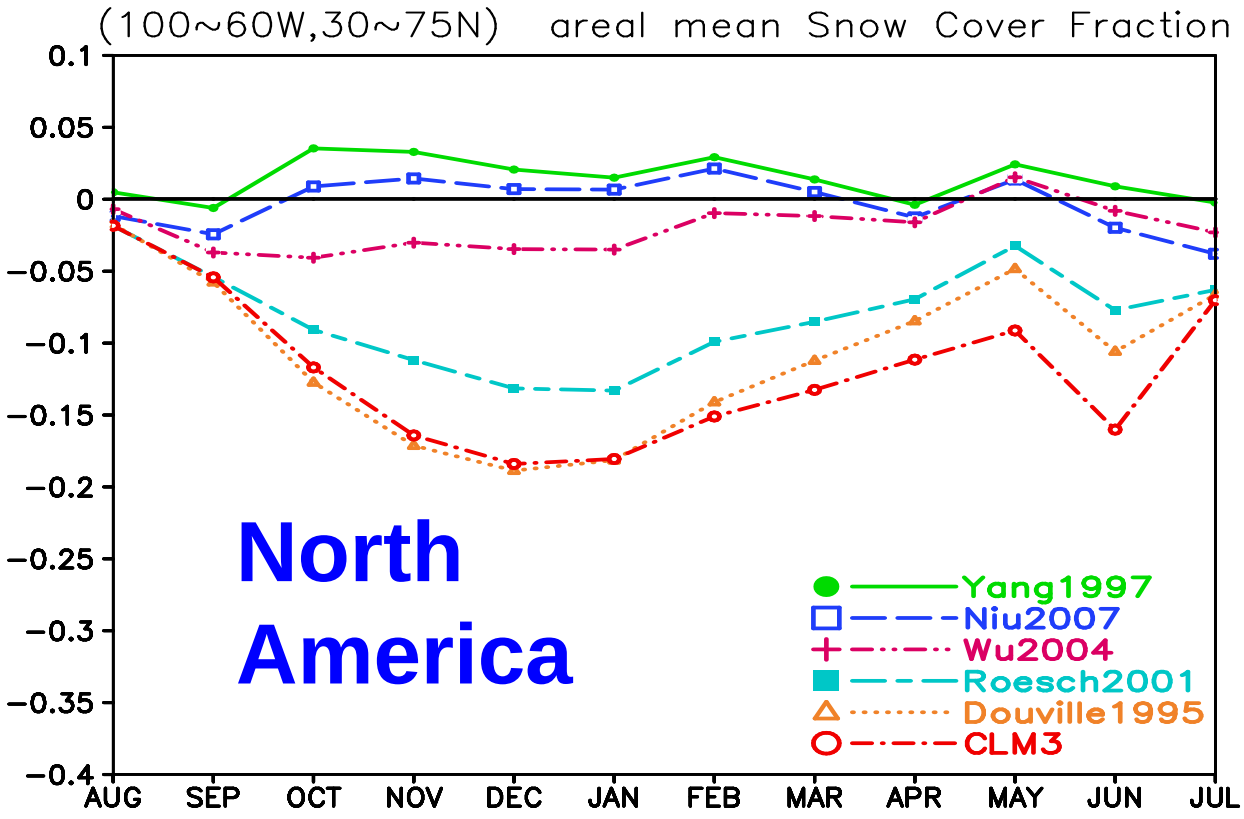

CLM3、Douville1995、Roesch2001: (–)

Yang1997: (+); Niu2007: (√)

SCF category	
1	$0.0 < SCF < 0.2$
2	$0.2 \leq SCF < 0.4$
3	$0.4 \leq SCF < 0.6$
4	$0.6 \leq SCF < 0.8$
5	$0.8 \leq SCF \leq 1.0$

Frequency distribution of SCF by category

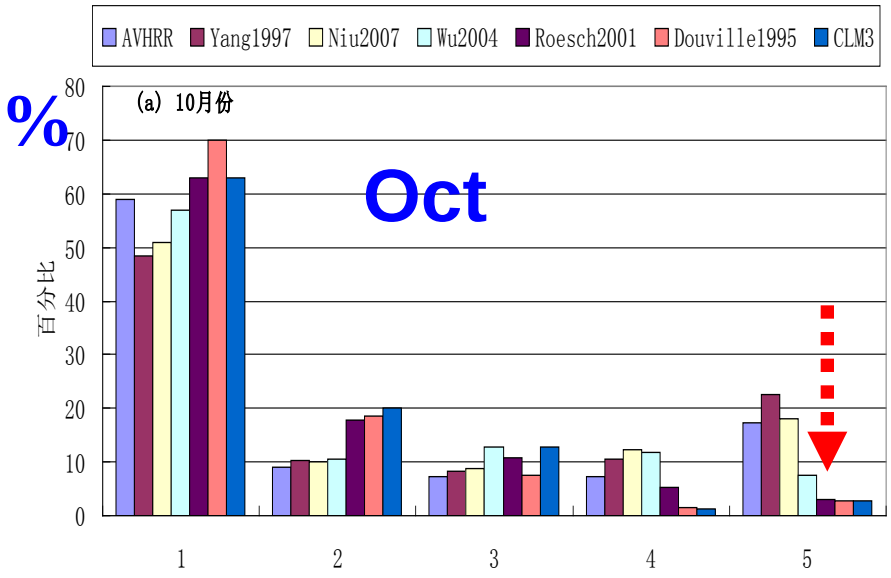

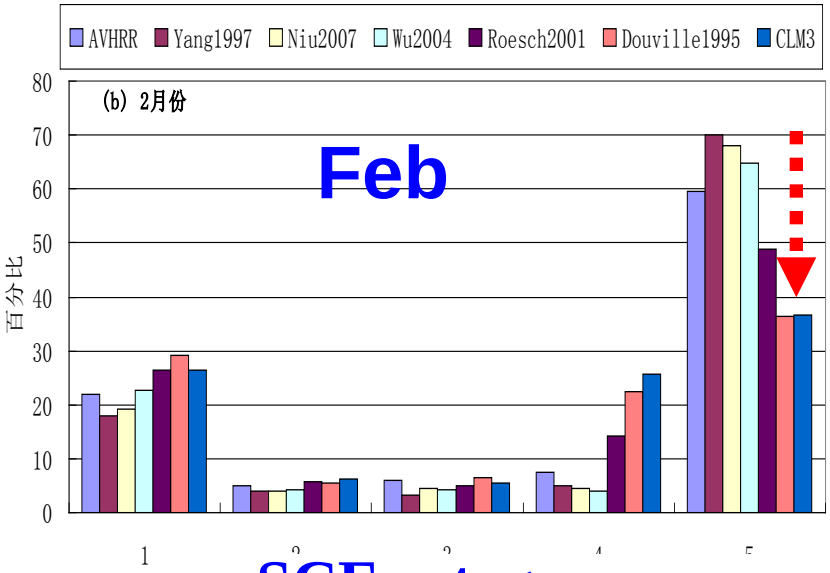

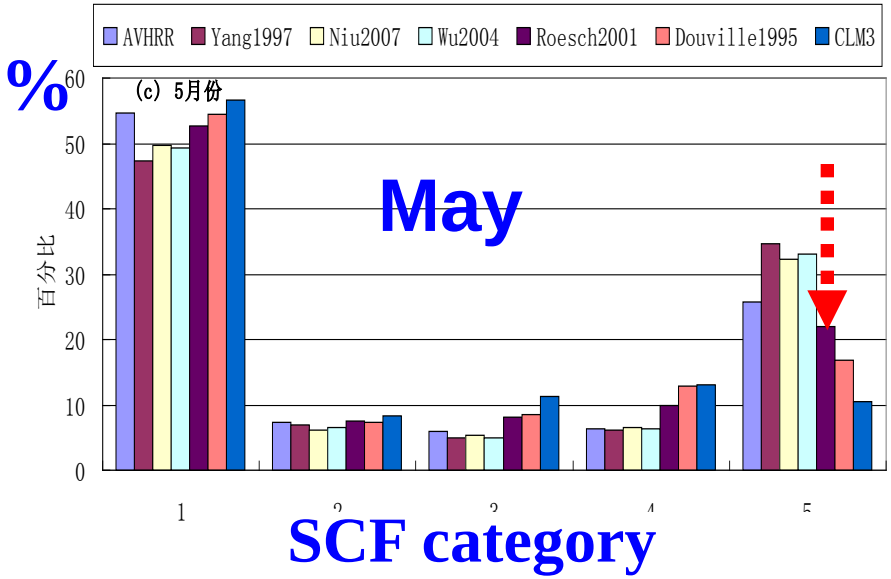

Roesch2001

Douville1995

CLM3

Less % in high SCF

Simulated SCF – AVHRR SCF in February

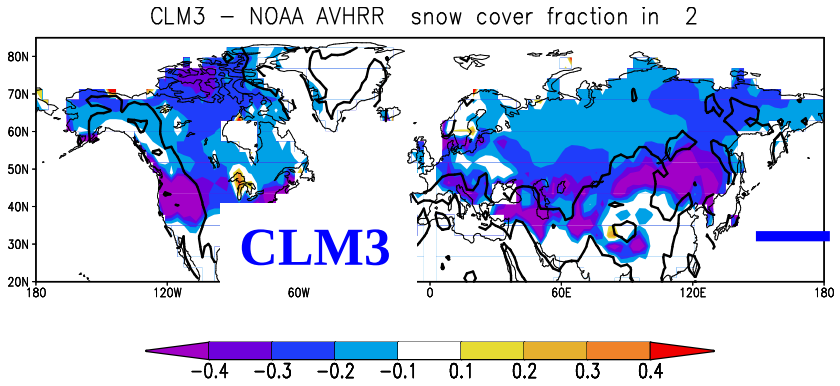

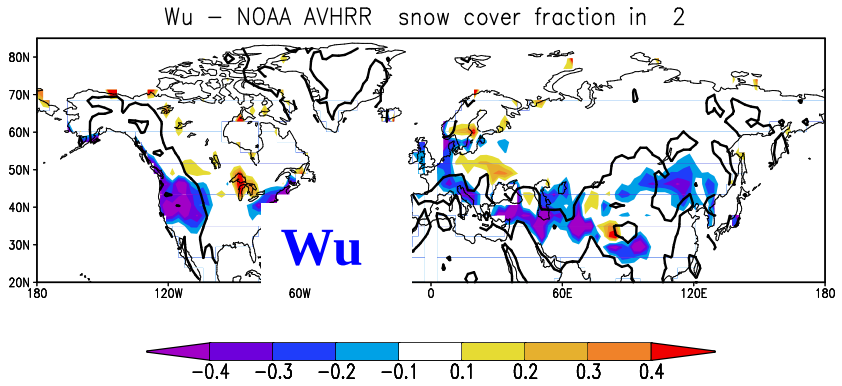

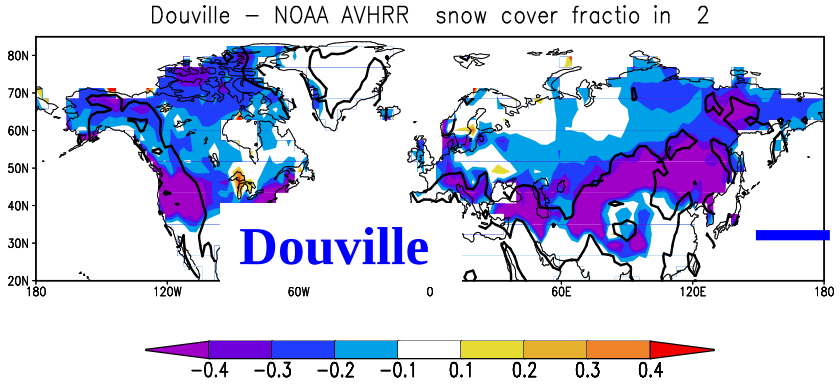

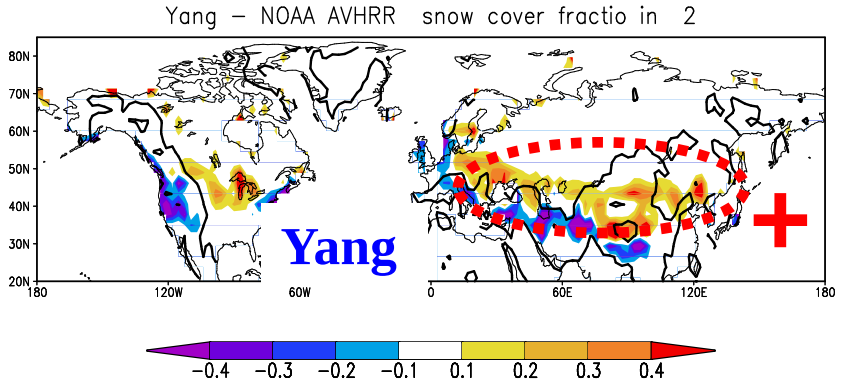

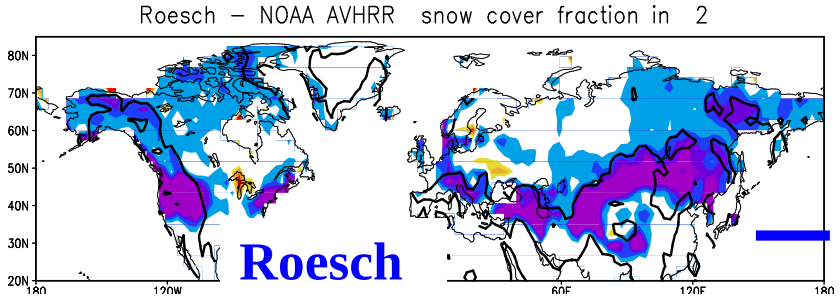

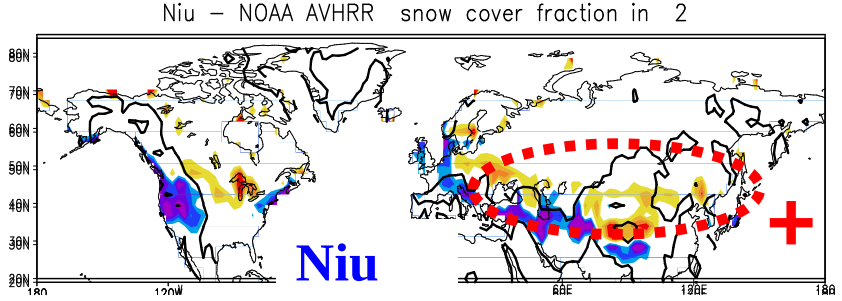

Standard deviation of topography

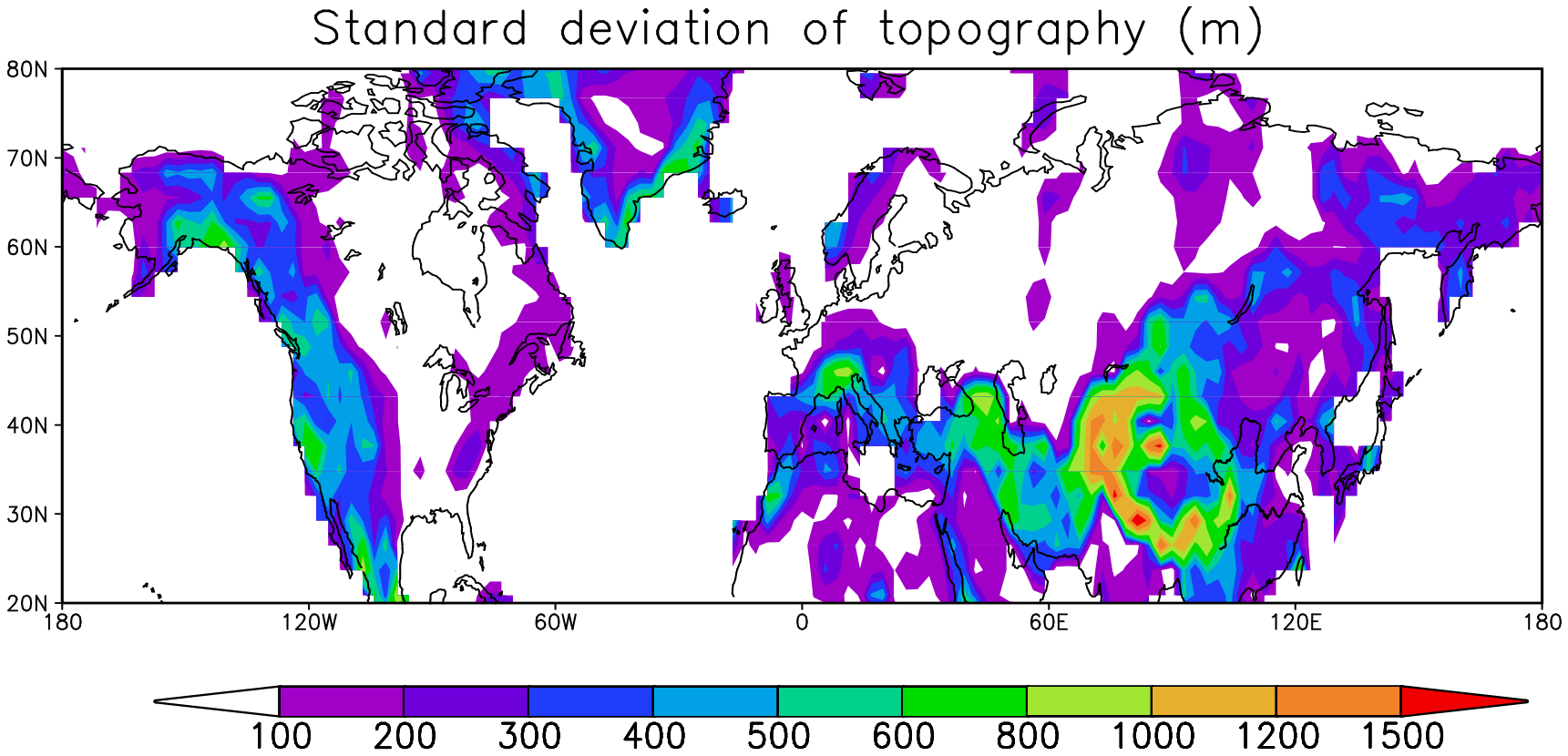

Modified SCF scheme

Roesch2001 $f_{sno} = 0.95 \tanh(0.1 \cdot s_n) \sqrt{\dfrac{s_n}{s_n + \varepsilon + 0.15\sigma_z}}$

Yang1997 $f_{sno} = \tanh\left(\dfrac{h_{sno}}{2.5 z_{0g}}\right)$

YR $f_{sno} = \tanh\left(\dfrac{h_{sno}}{2.5 z_{0g}}\right) \sqrt{\dfrac{s_n}{s_n + \varepsilon + 0.01\sigma_z}}$

Simulation SCF – MODIS SCF

YR – MODIS

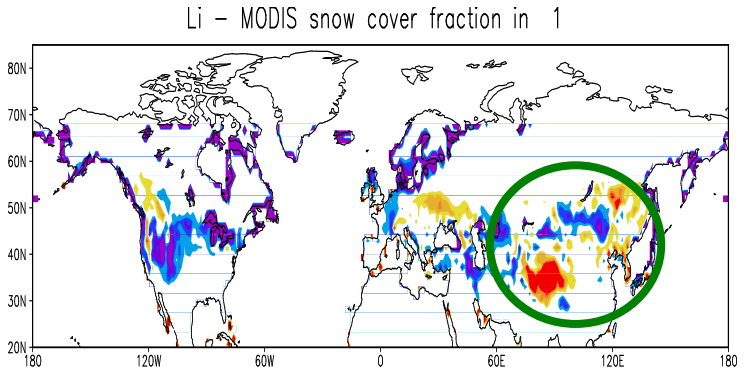

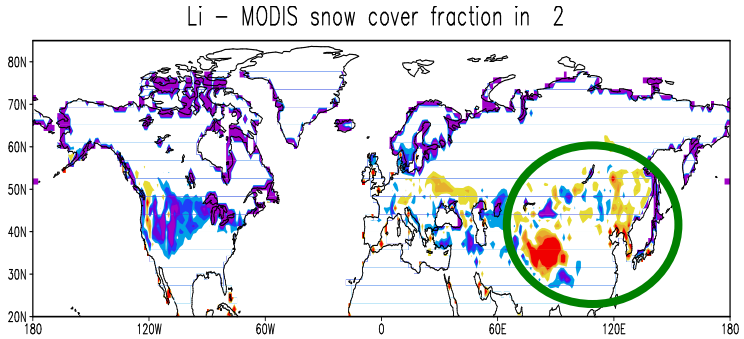

Niu2007 – MODIS

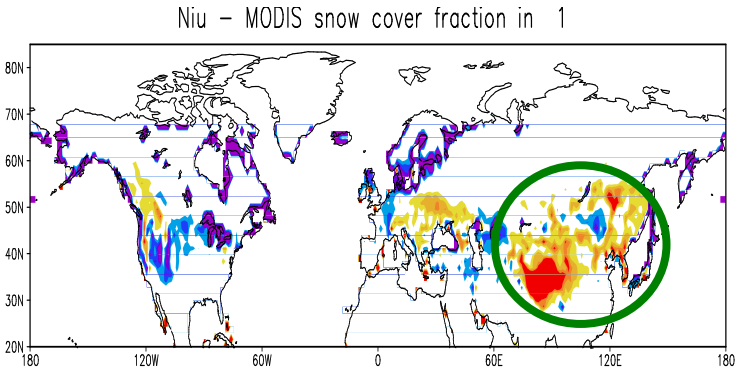

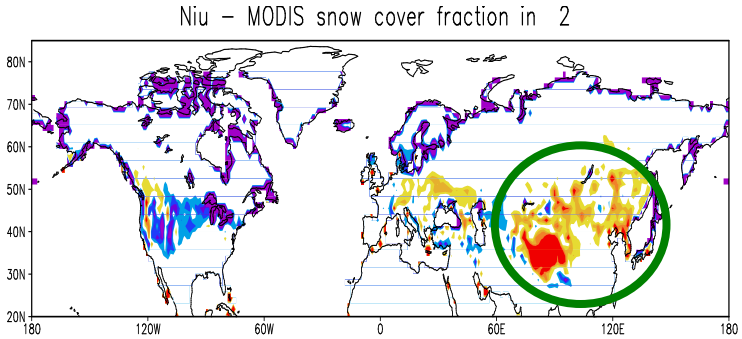

Jan

Feb

Smaller +bias over Tibetan-Mongolian Plateau areas in modified YR scheme

4. summary

Under the framework of CLM3

- CLM3、Douville1995、Roesch2001: less SCF
- Yang1997: more SCF along southern border
- Niu2007: alleviate +bias in Yang1997

  +bias still exist in mountainous areas

Considering sub-grid orography variation alleviate the +bias in Yang1997

4. Discussion

The essence of SCF<1 is mainly due to heterogeneity within a GCM grid (topography, wind, snowfall).

- In Niu2007 (CLM4) scheme, snow density is already represented by snow depth, no additional information is provided by double considering snow density.
- Orientations of topography influence snowfall, radiation, therefore affect SCF, which should be considered in future SCF scheme.

Outline

Part II: Frozen Soil

1. Background
2. Data, Experiment
3. Results
4. Summary

1. Background

- globe (23%land：permafrost)
- Northern Hemisphere (winter: 55-60%)
- China (21%, 53.3%, 23.9%)

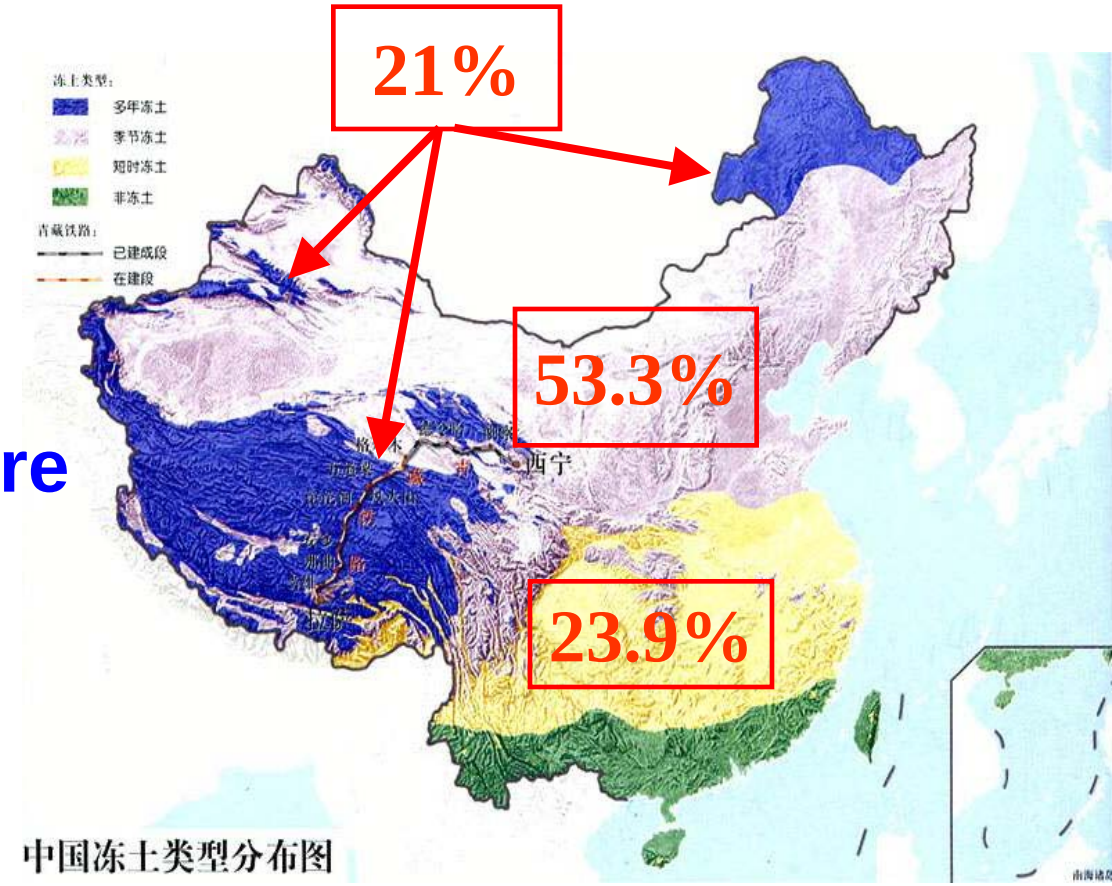

China National Geography，2004

Properties of Frozen Soil

In comparison to soil liquid water

1. **Soil ice has smaller hydraulic conductivity，hence less infiltration，more surface runoff**
2. **Soil ice has larger thermal conductivity, but smaller heat capacity, diurnal and seasonal temperature fluctuation can transfer to a deeper soil layer.**

	thermal conductivity	heat capacity
water	0.57 $Wm^{-1}K^{-1}$	4.19 $\times 10^6$ $J\ m^{-3}K^{-1}$
ice	2.29 $Wm^{-1}K^{-1}$	1.94 $\times 10^6$ $J\ m^{-3}K^{-1}$

3. **Heat release/absorption associated with freeze/thaw**

Frozen soil schemes in Climate models

1. No freeze-thaw, modified hydraulic/thermal properties.

SSiB (Xue et al., 1991), BATS (Dickinson et al., 1993)

2. Freeze-thaw, soil ice content changes with available energy

BASE (Slater et al.,1998)

CCSR/NIES GCM (Takata and Kimoto, 2000)

NCAR CLM3 (Dai et al., 2003) (freeze at 0°C)

3. Maximum soil water content after freezing

Eta model (Koren et al., 1999)

VIC (Variable Infiltration Capacity) (Keith et al., 1999)

NCAR CLM4 (Niu and Yang, 2006) (freeze below 0°C)

When ice is present，soil water potential remains in equilibrium with the vapor pressure over pure ice, soil water matric potential is:

$$\psi(T) = \frac{10^3 L_f (T - T_{frz})}{gT}$$

Freezing-thawing is similar to drying-wetting process with regard to ψ and θ

(Spaans and Baker, 1996) ：

$$\psi(\theta_{liq}) = \psi_{sat} \left(\frac{\theta_{liq}}{\theta_{sat}} \right)^{-b}$$

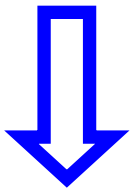

Threshold temperature when soil water begin to freeze at certain θ

$$T_{crit} = \frac{10^3 L_f T_{frz}}{10^3 L_f - \psi_{sat} \left(\frac{\theta_{liq}}{\theta_{sat}} \right)^{-b} g}$$

T_{frz} and soil water content for different soils

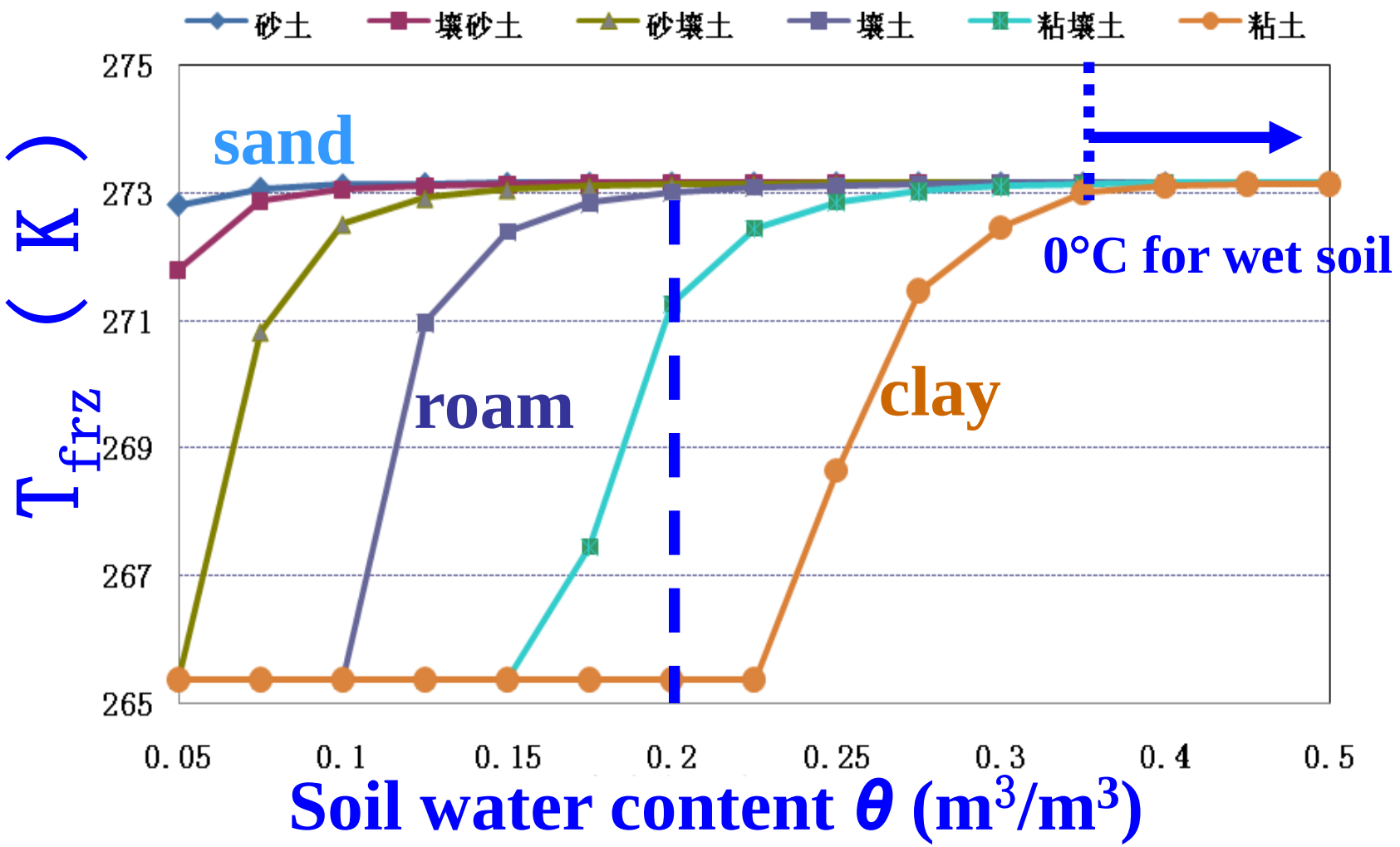

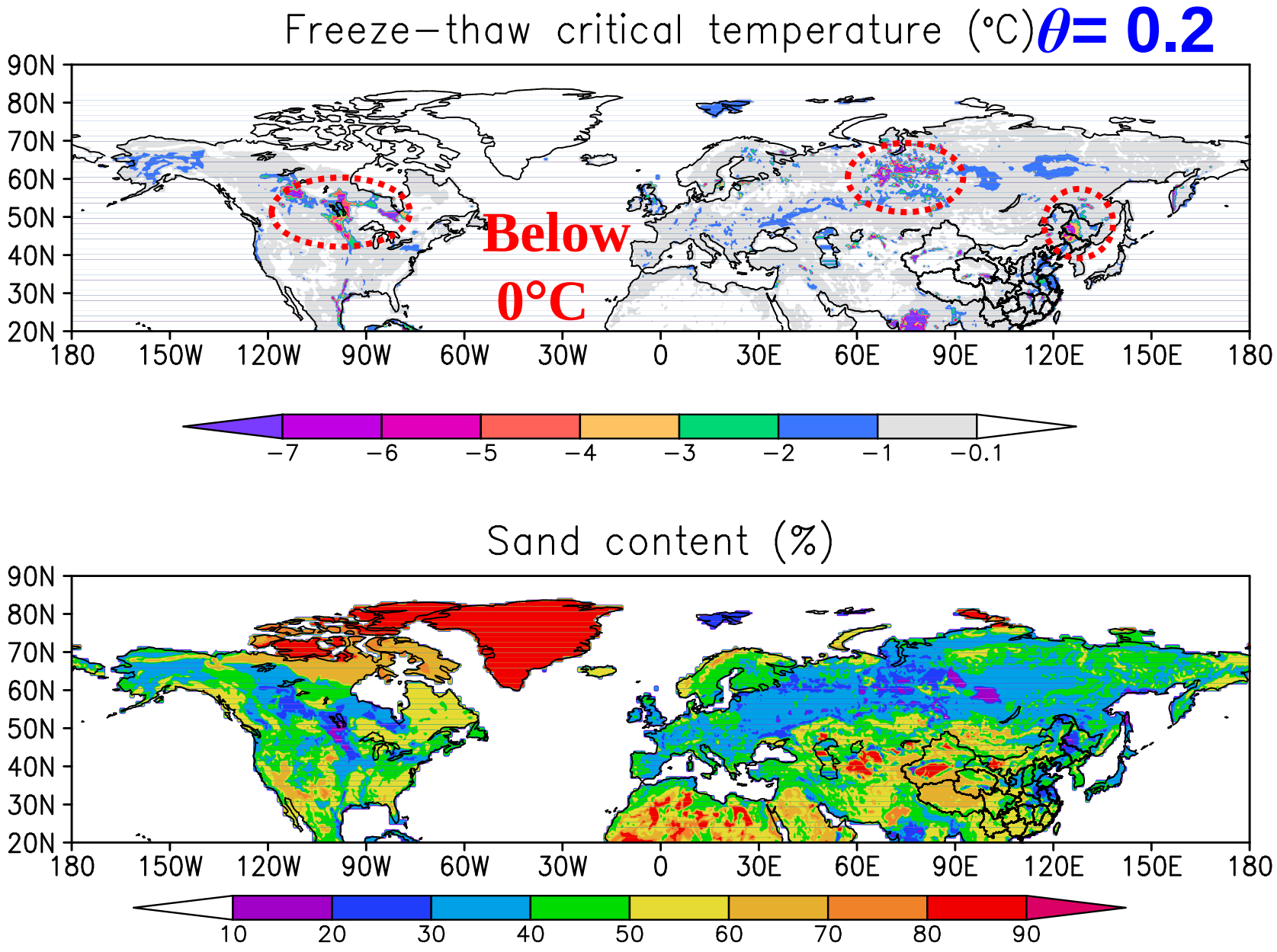
Freeze−thaw critical temperature (°C) θ= 0.2
90N
80N
70N
60N
50N
40N
30N
20N
180
150W
120W
90W
60W
30W
0
30E
60E
90E
120E
150E
180
Below
0°C
−7
−6
−5
−4
−3
−2
−1
−0.1
Sand content (%)
10
20
30
40
50
60
70
80
90

2. Observation Data

Suli station (38.42°N, 98.30°E, 3802 m), northeast Tibetan Plateau, Sandy soil covered by cold grass

Variables：Tair、pressure、humidity、wind、precipitation、radiation

soil temperature at 5cm, 10cm, 30cm, 50cm, 70cm
soil moisture at 20 cm, 40 cm, 60 cm

Data span: February 1, 2009 ~ December 31, 2009

run CLM3 offline （single point）

Observation of Suli Station over Tibet

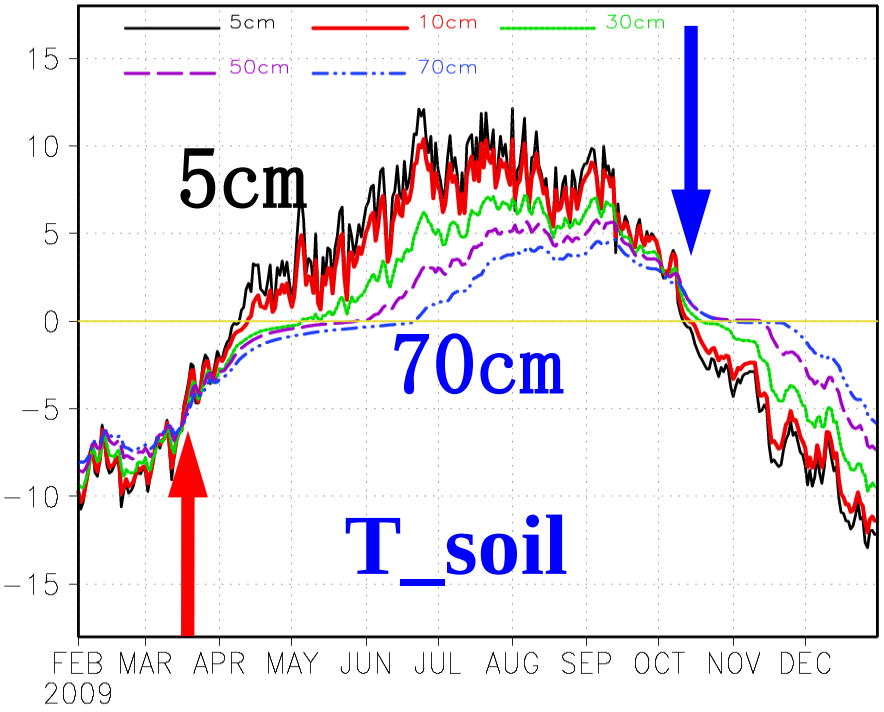

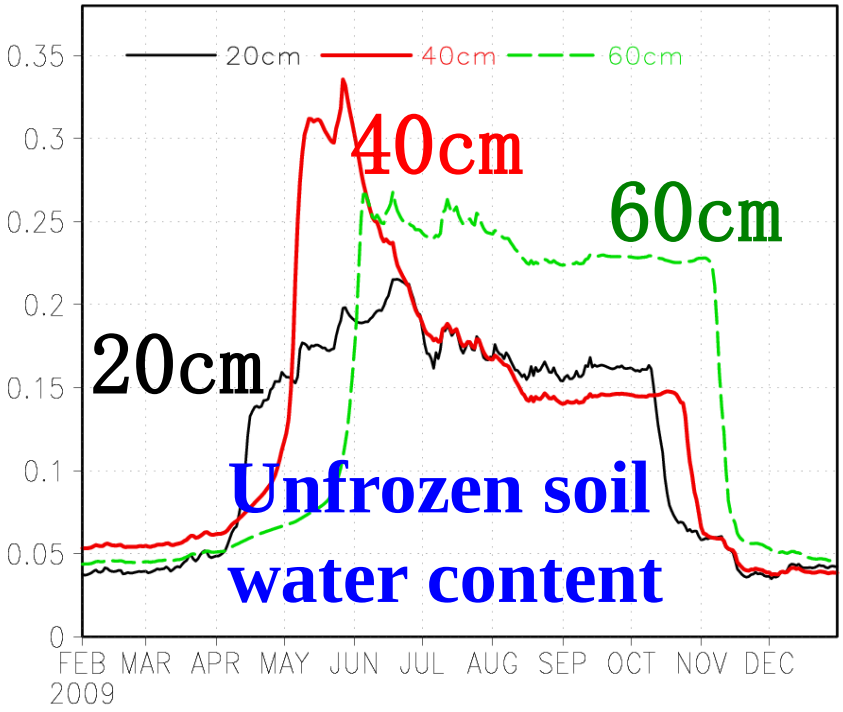

The seasonal evolution of soil temperature at different vertical layers

Later thawing/freezing of soil water in deeper layer

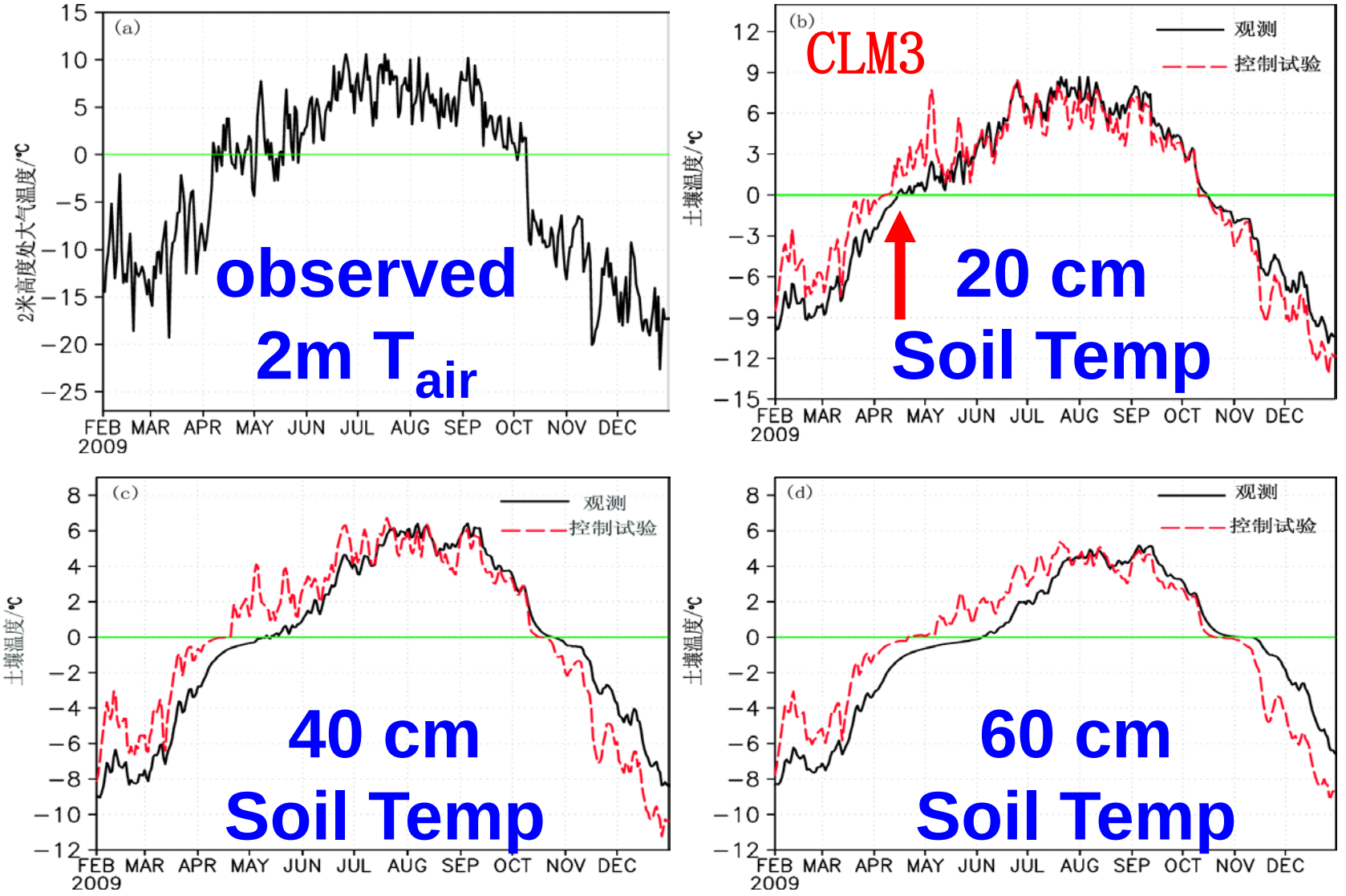

Early completely thawing in CLM3 (0°C scheme)

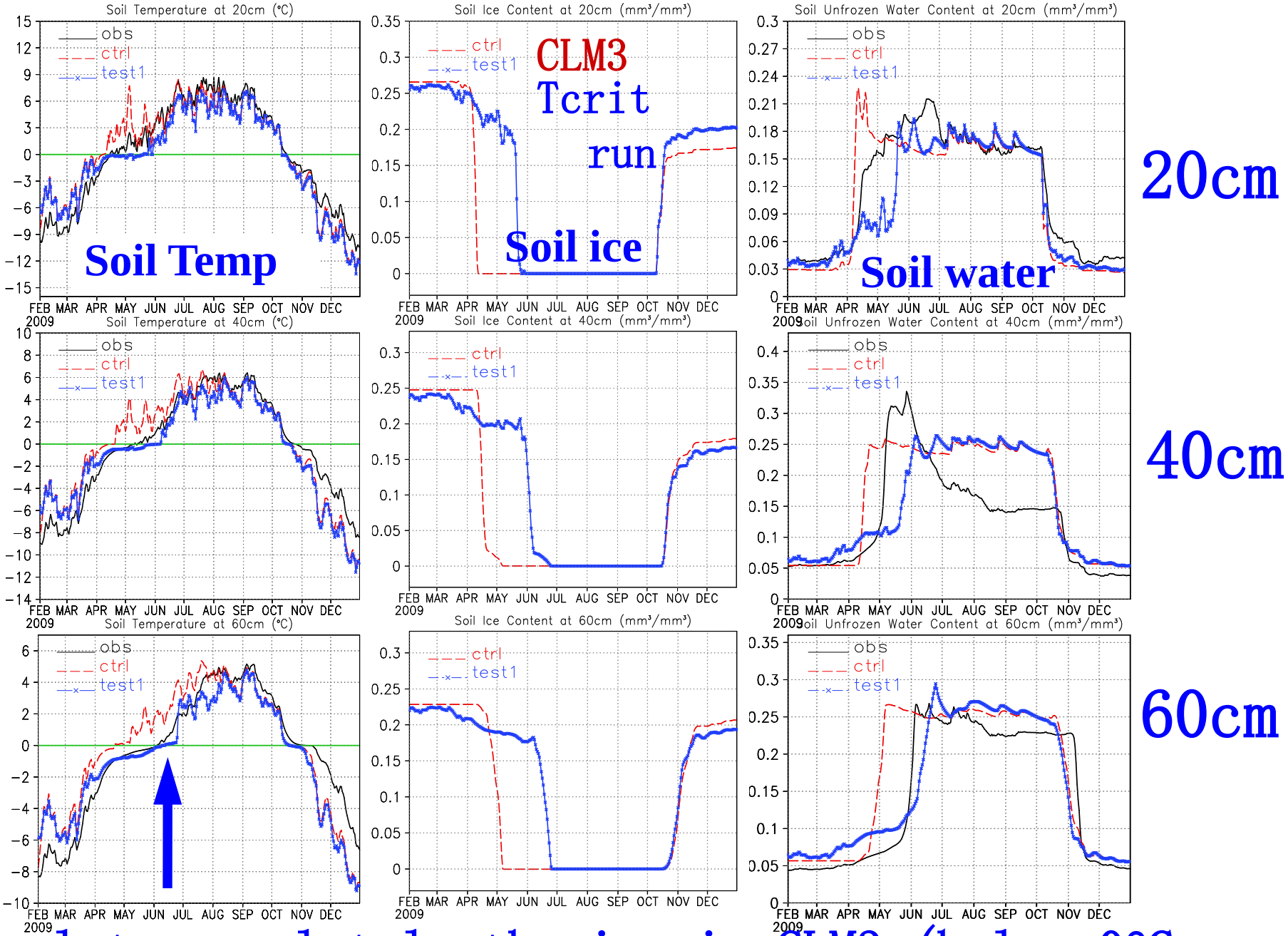

late completely thawing in CLM3 (below 0℃

Global simulation

CLM3 offline run

new scheme: freezing below 0°C

old scheme: freezing at 0°C

Forcing: Qian 2006 (NCEP) (1980-2004)

1985-2004 20-year average

after 5-year initialization

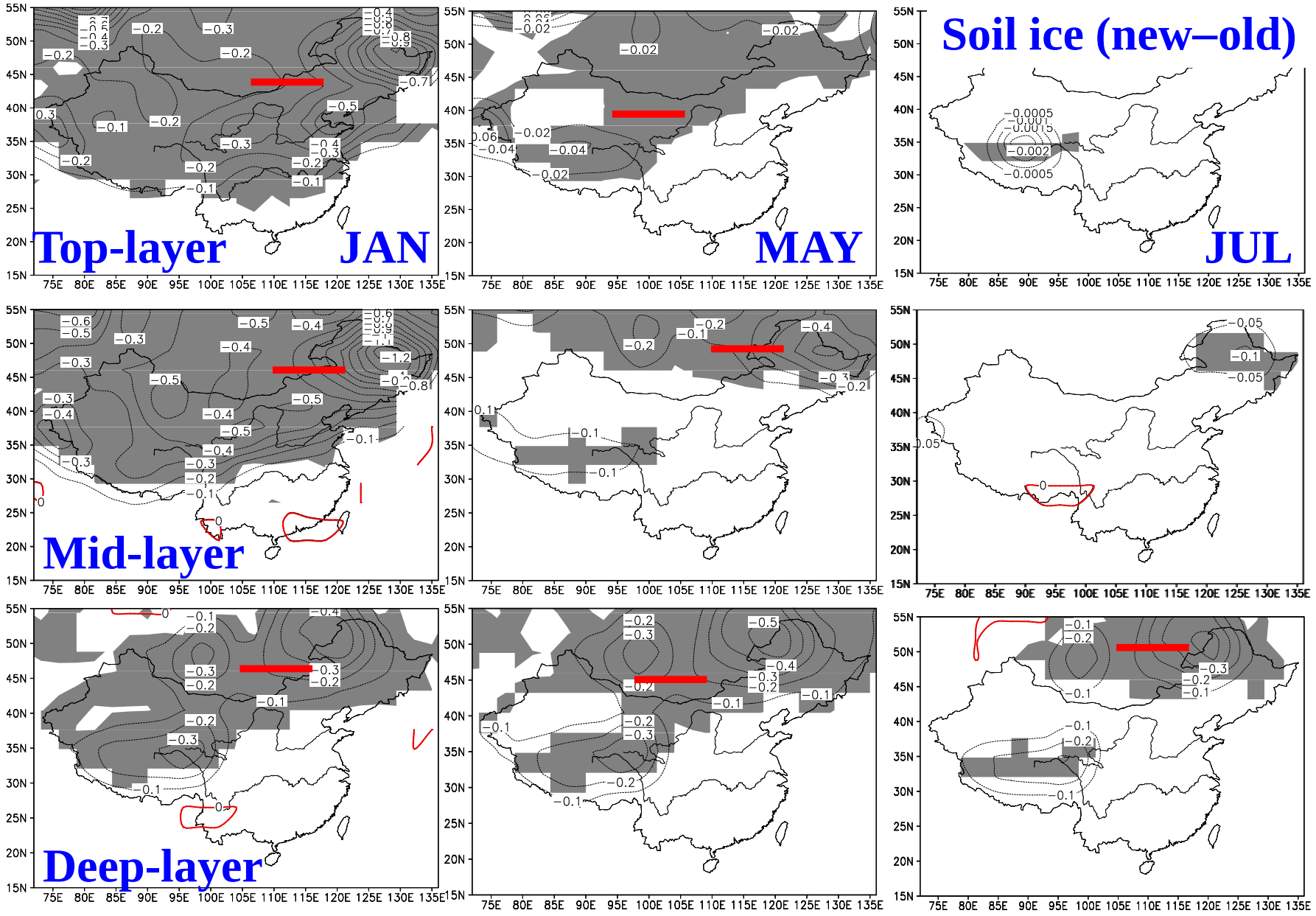

Less soil ice when supercooled water is allowed. shading: 90% confidence level

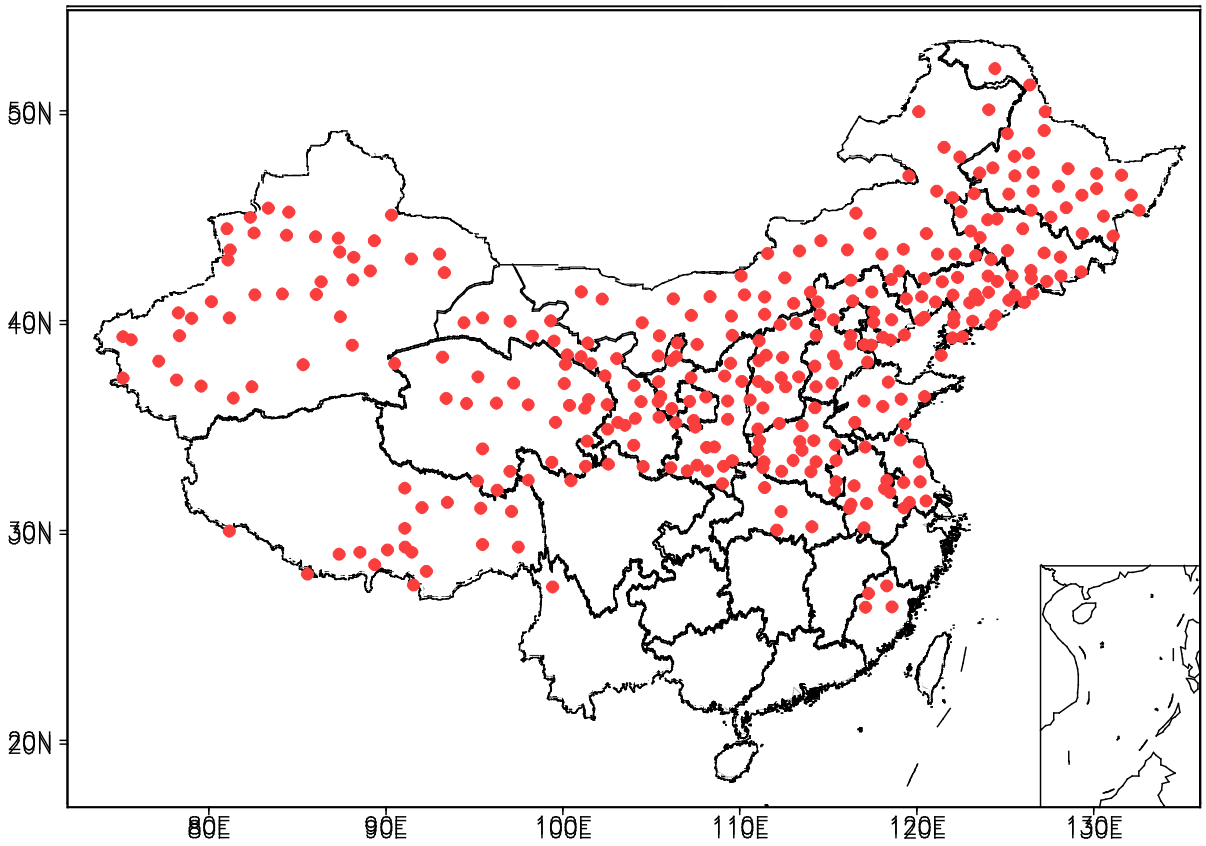

Stations with observations of soil frozen depth in China

0°C scheme

OBS

Below 0°C scheme

DEC

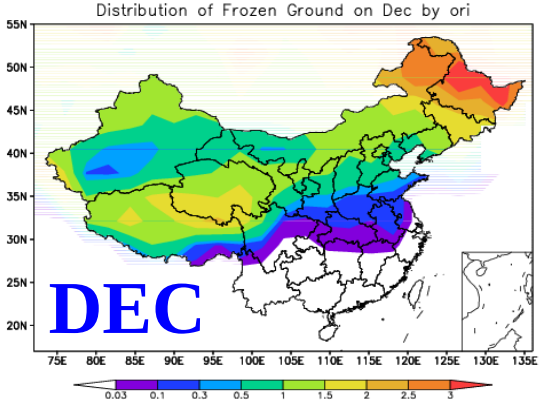

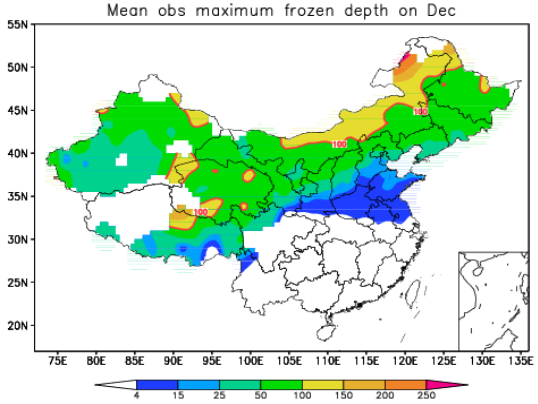

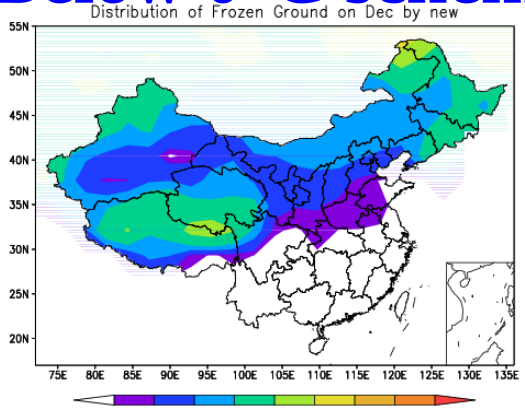

JAN

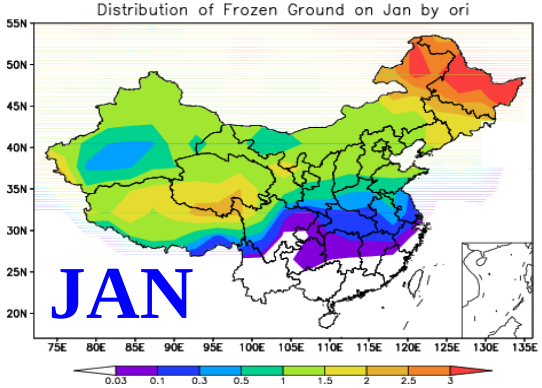

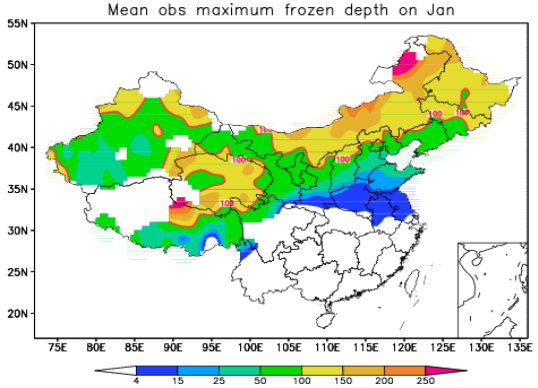

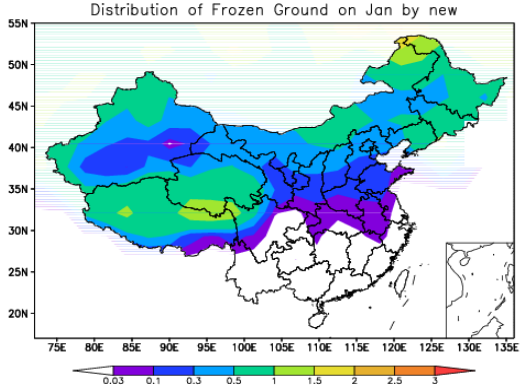

FEB

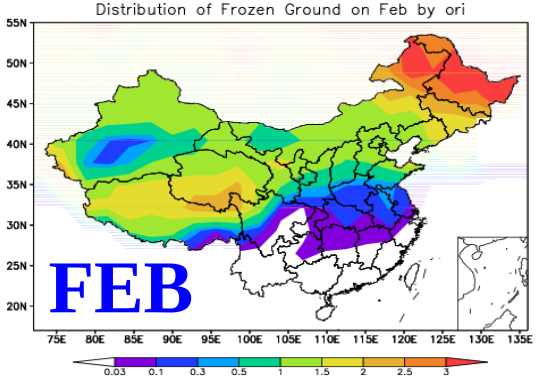

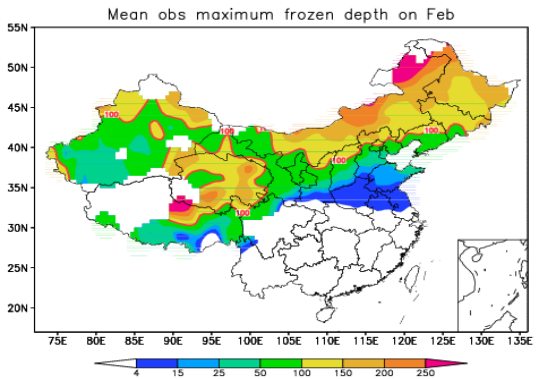

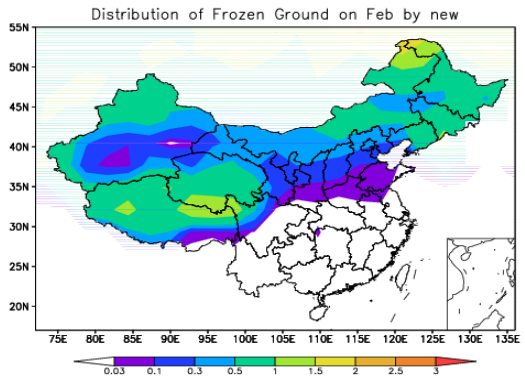

4. Summary

1) Soil water begin to freeze at a sub-freezing temperature under relatively dry condition, depending on soil characteristics. The higher soil clay percentage, the lower the freezing temperature is. This threshold is close to 0°C for saturated soil, which is the default situation in CLM3.

2) In spring, when soil ice begin to melt at a lower than 0°C temperature, thawing consumed heat and larger than ice heat capacity of melt water impede the increase of soil temperature. In autumn, freezing process is postponed in the new scheme when supercooled water is allowed to coexist with soil ice.

3) The modified scheme did better simulation of frozen soil distribution and its seasonal evolution in China.

Thank You !

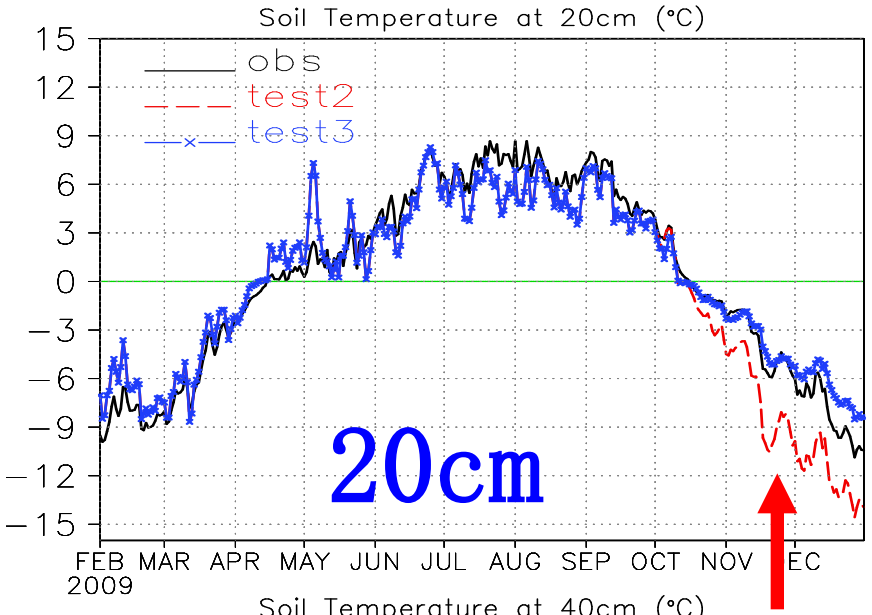

Simulation of soil Temp further improved

By reducing freezing rate in autumn

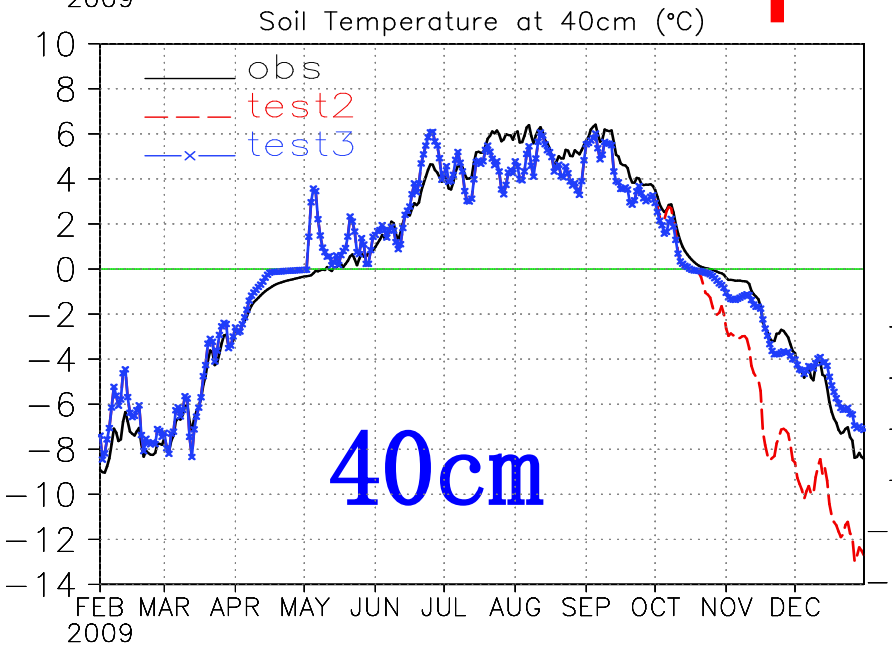

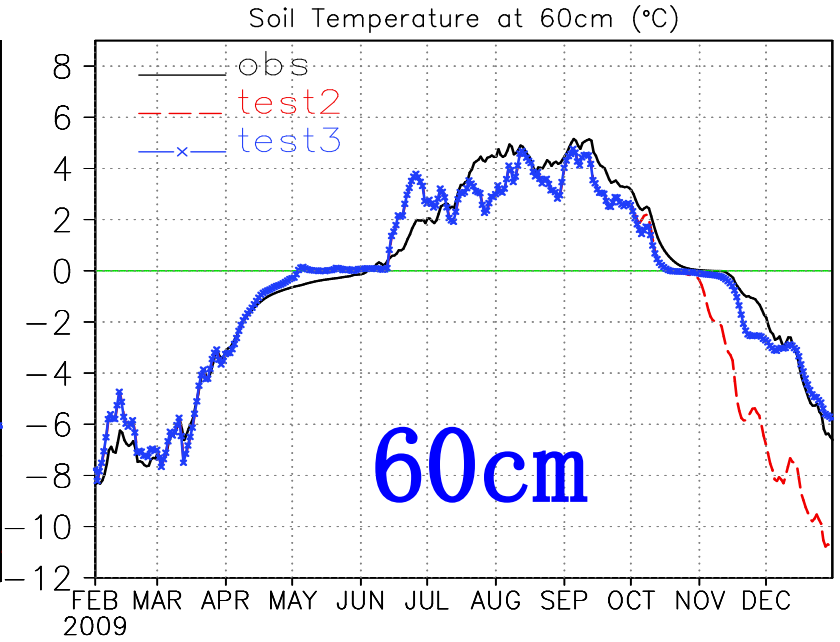

Difference in surface net longwave Radiation (W/m2) (new - old)

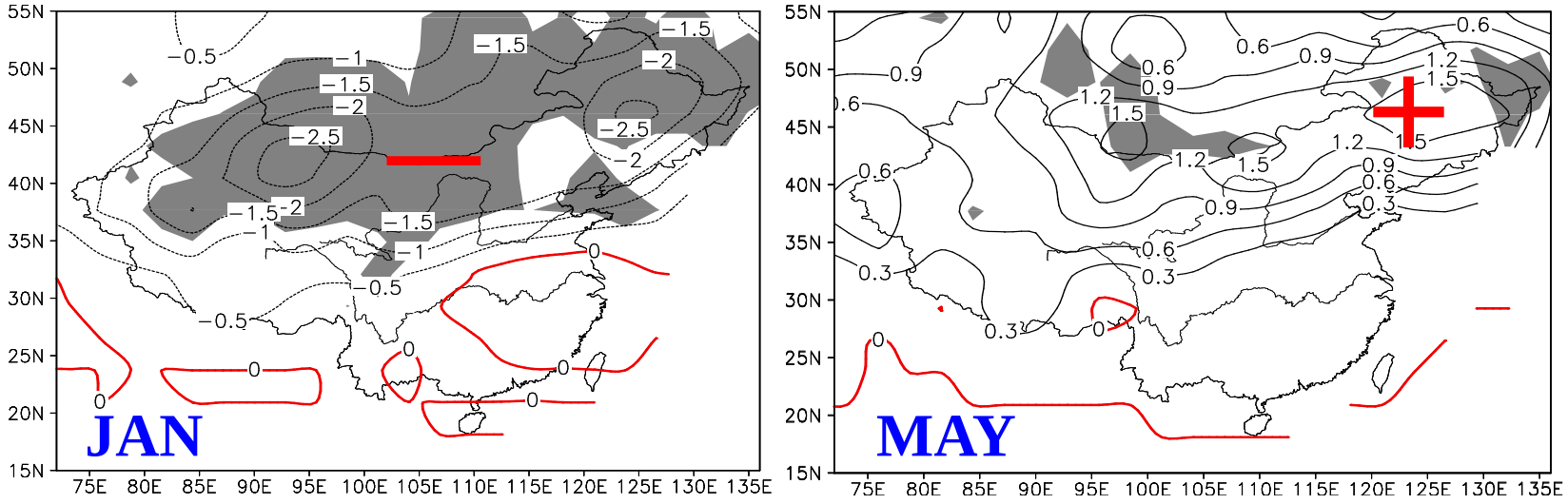

Difference in surface net SW (W/m2) (new －old)

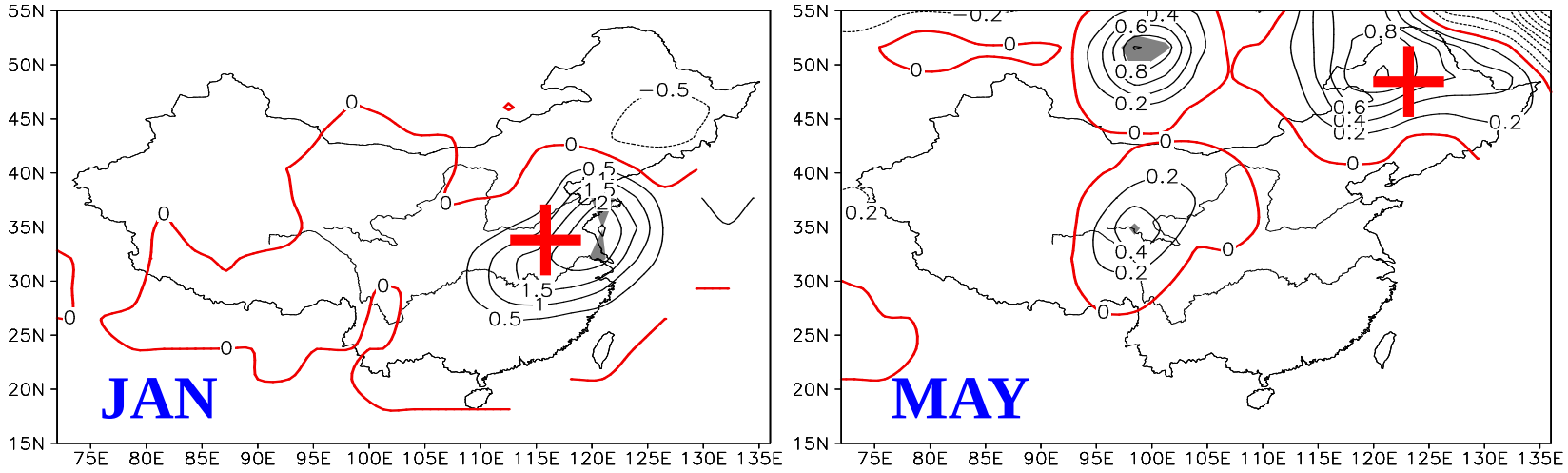

Sensible heat flux（W/m2） （new －old）

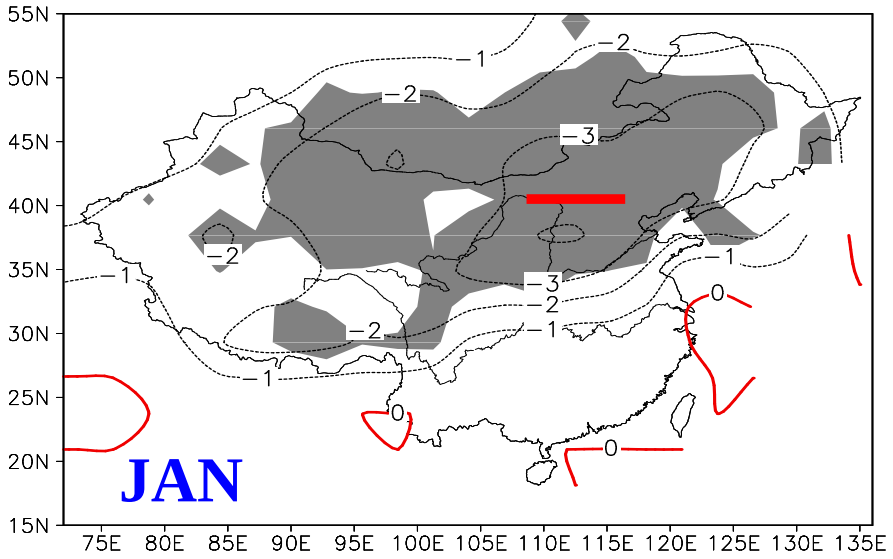

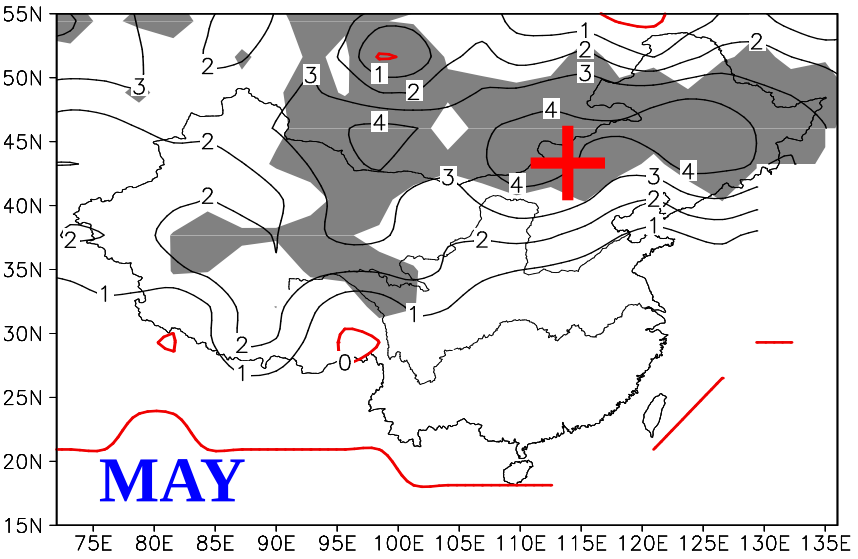

Latent heat flux（W/m2）

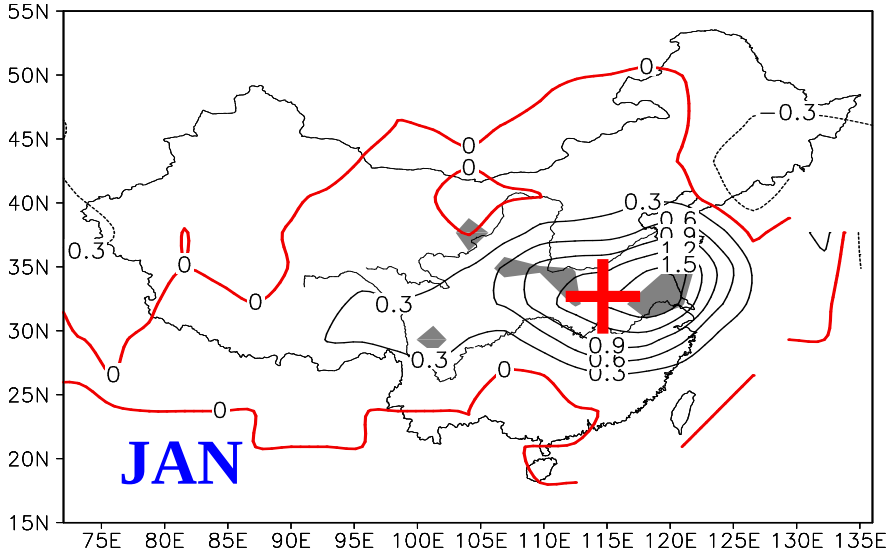

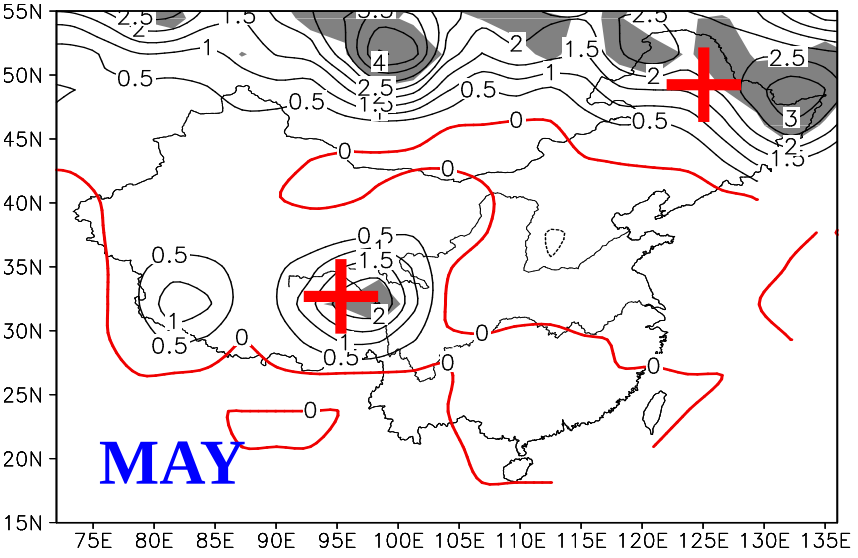

Difference in Ts（℃）simulation（new －old scheme）

（shading： 90% confidence level）

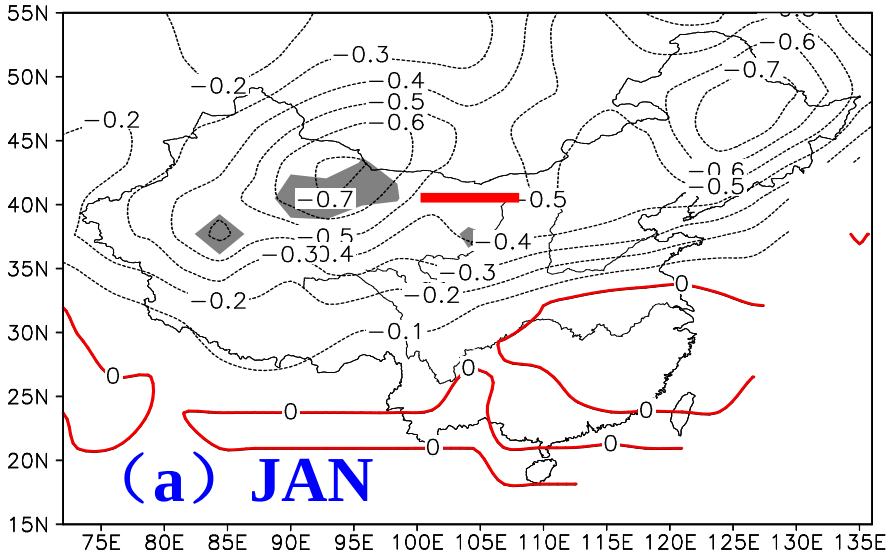

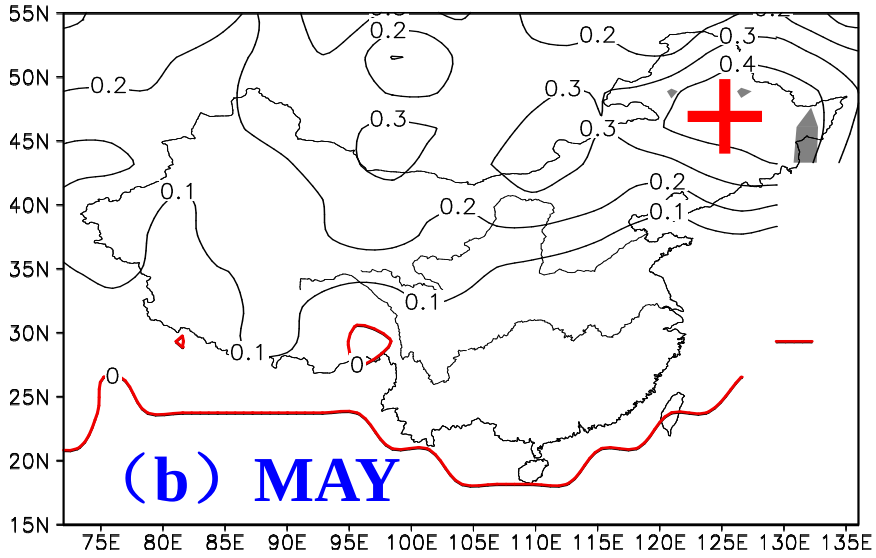

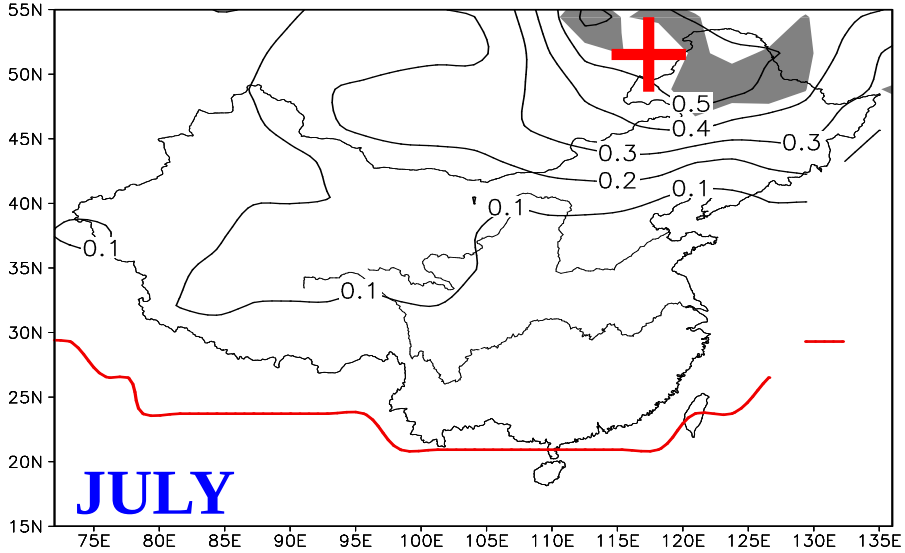

CAM3-CLM3 coupled simulation of soil ice content (new－old)

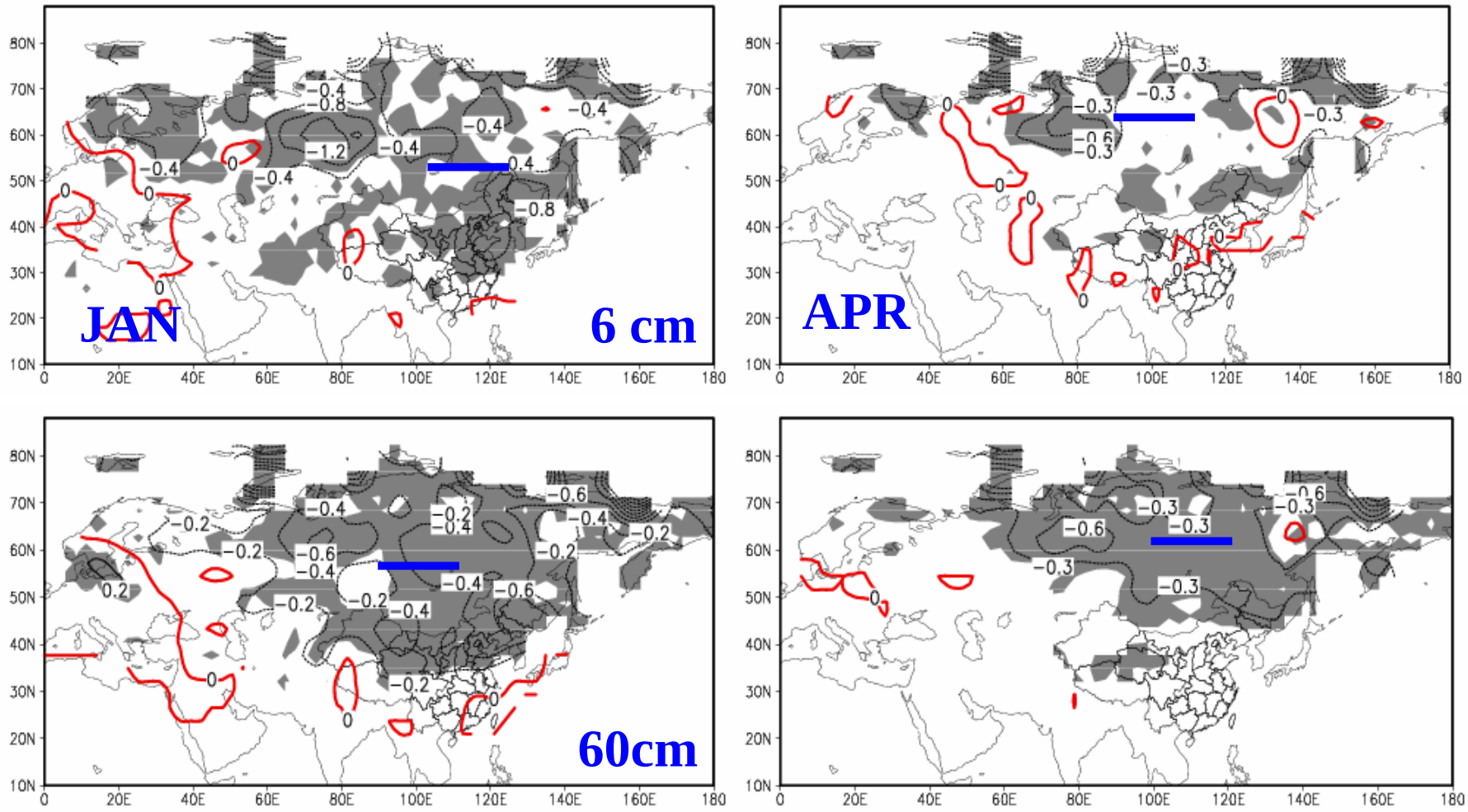

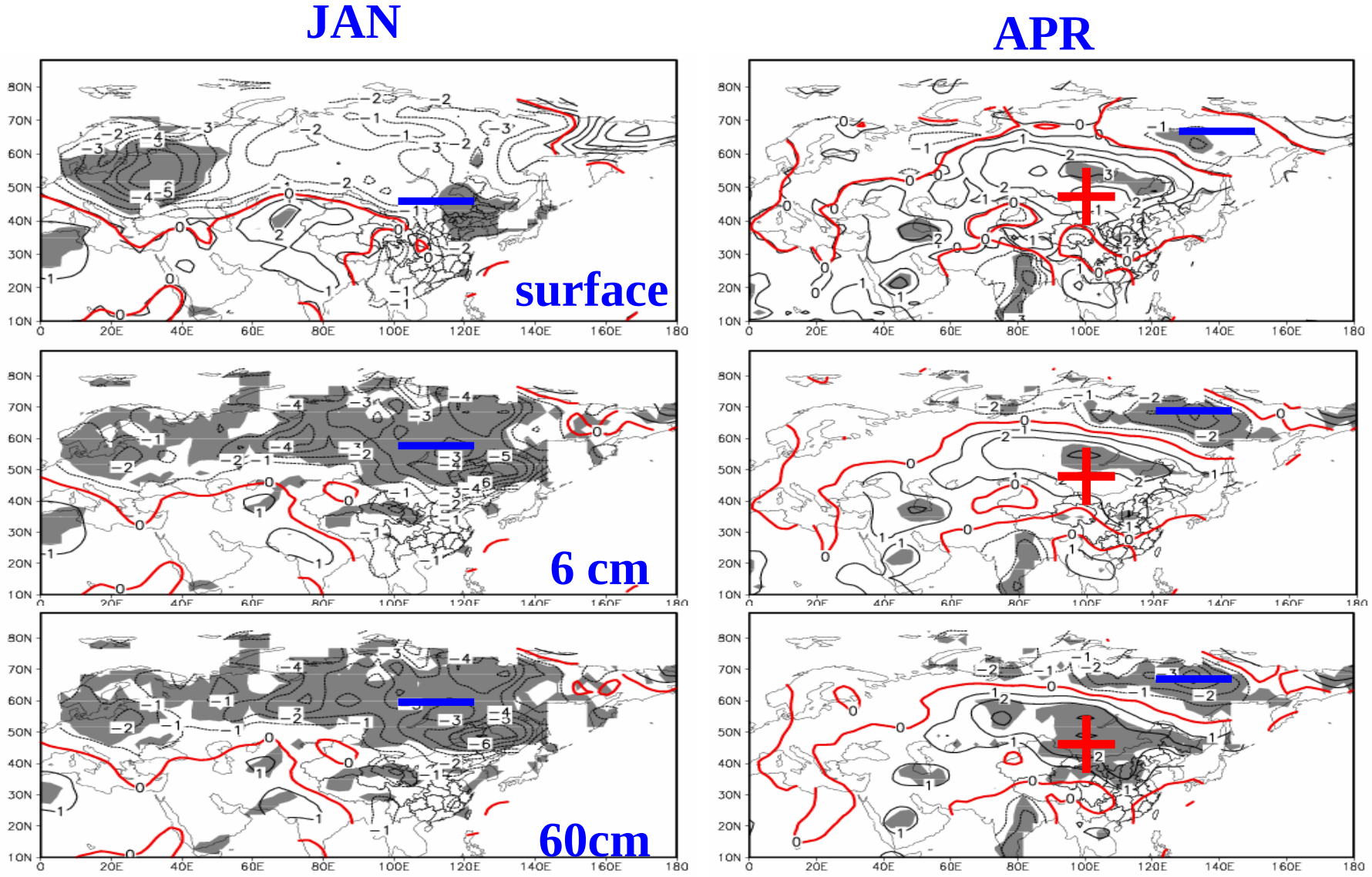

new－old simulation of soil temperature (℃)

New －old surface sensible heat flux（W/m2 ）

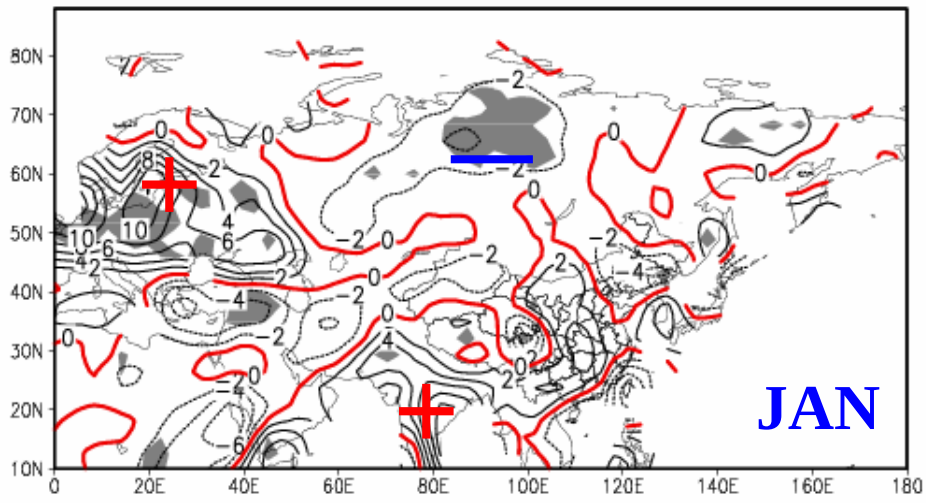

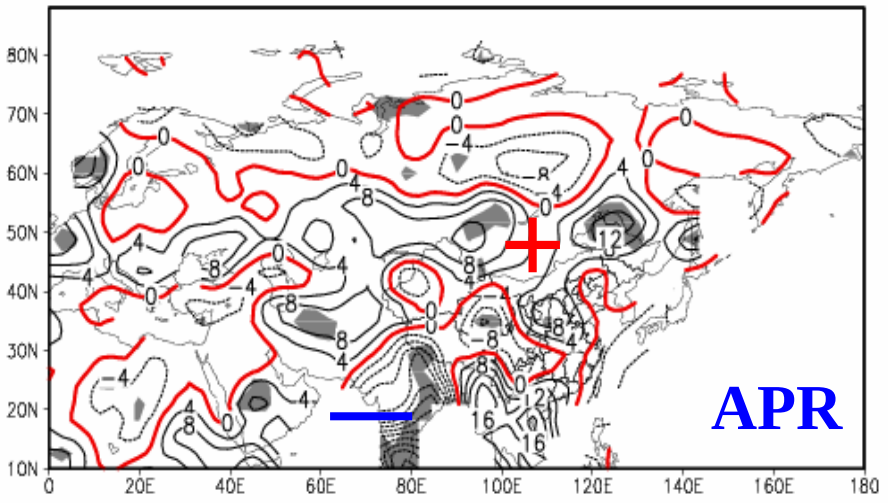

New －old surface latent heat flux（W/m2 ）

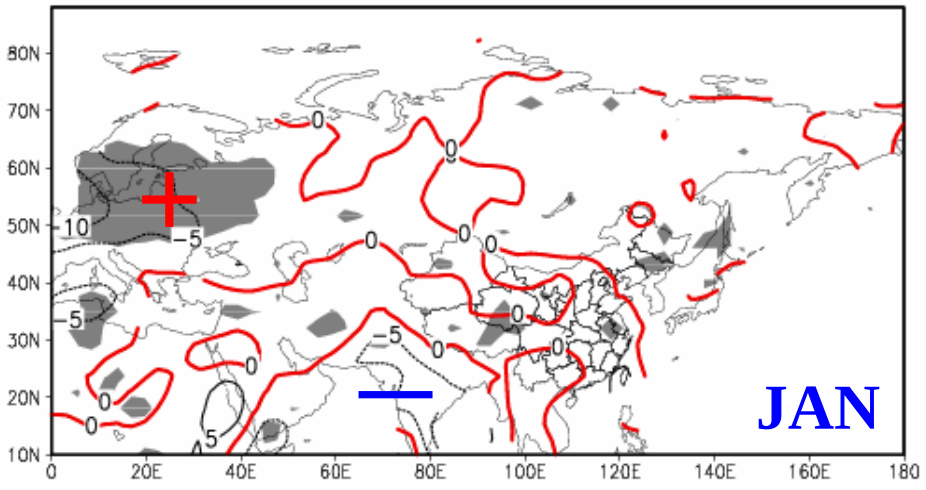

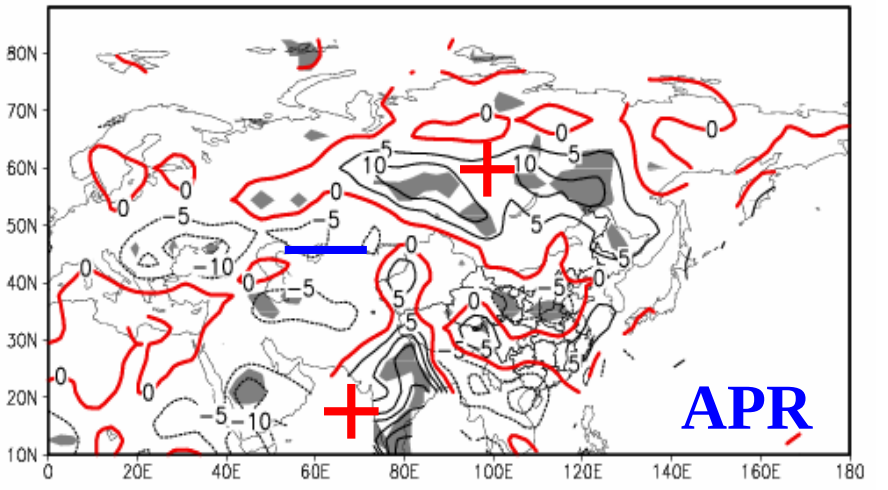

Simulated SCF – AVHRR SCF in November

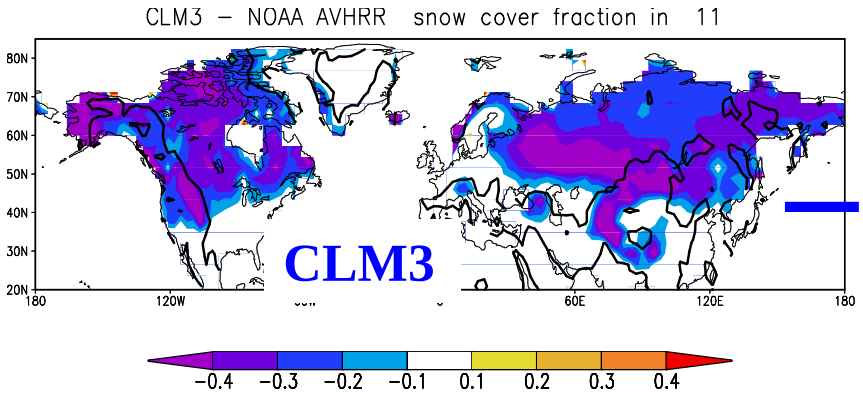

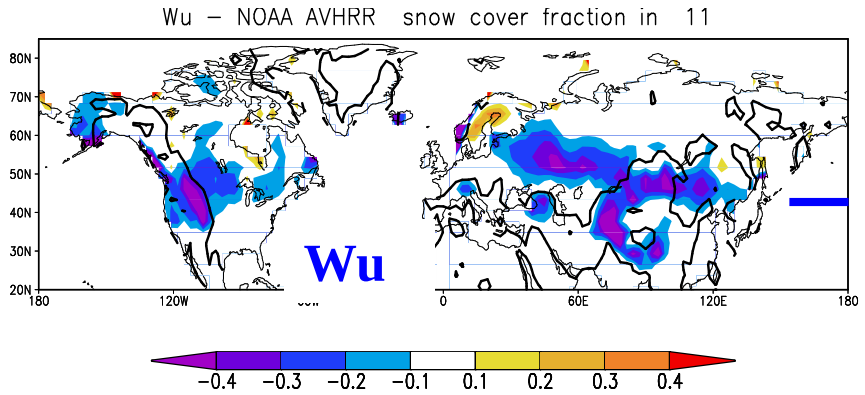

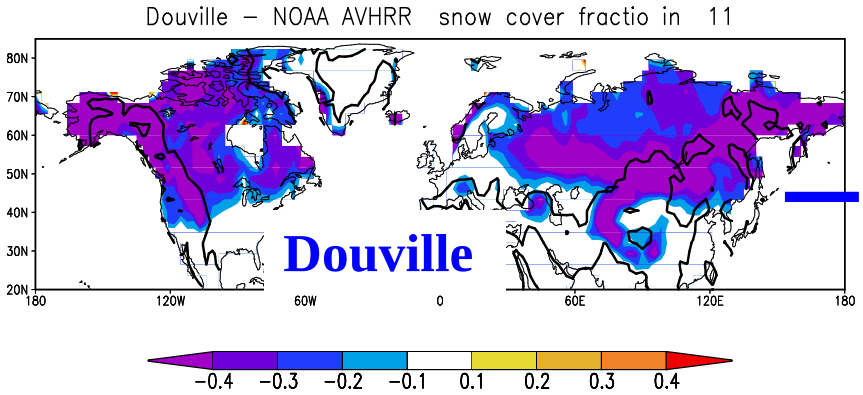

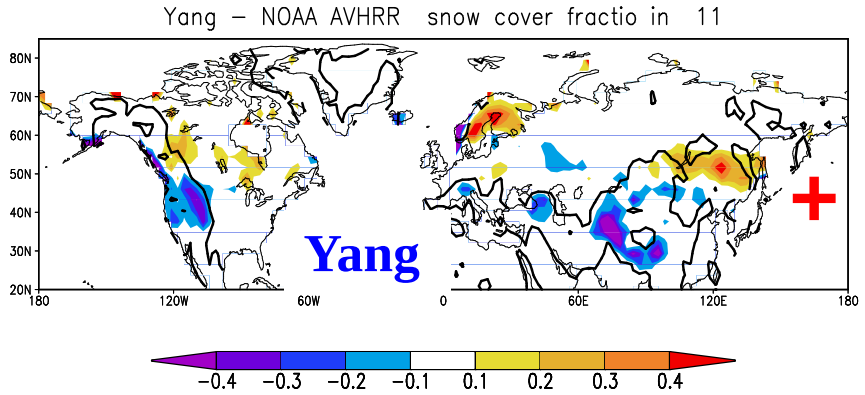

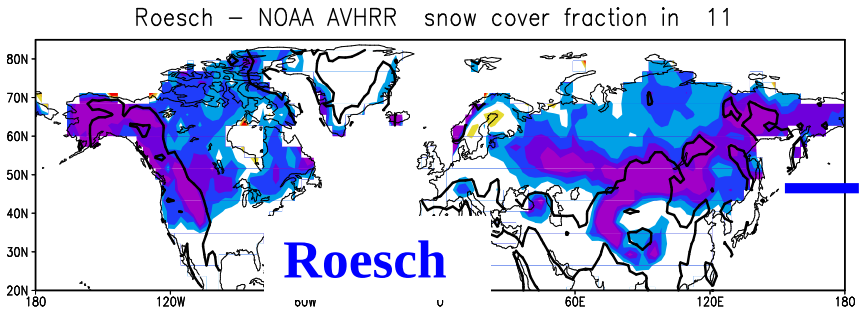

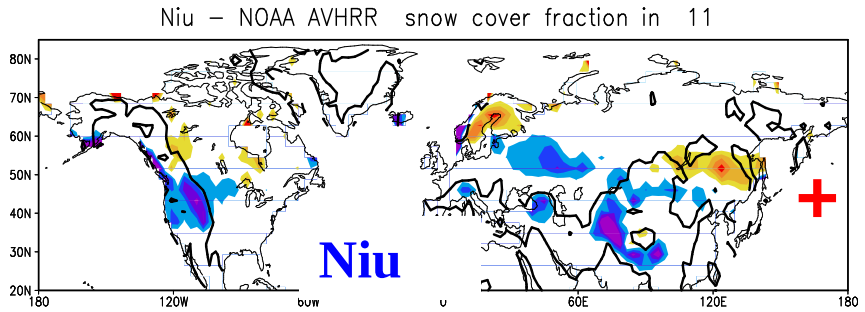

% increase in monthly precipitation over NW NA for PRISM (Daly, 2002) and Adam(2006) orographically corrected data

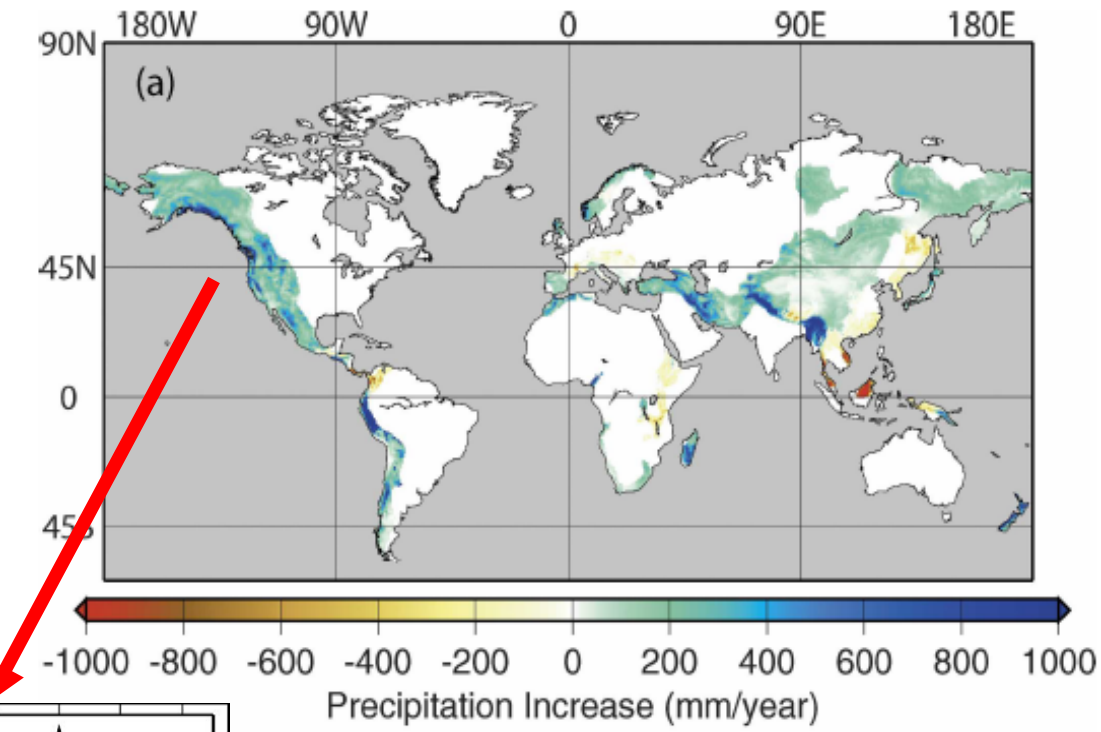

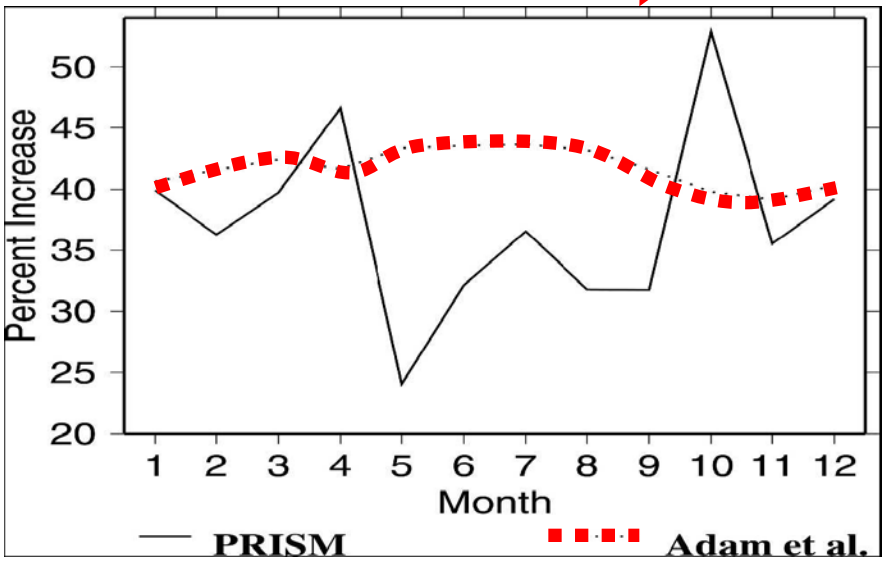

Continent	Precipitation increase Correction domain only
Africa	7.4
Australia	6.2
Eurasia	20.3
North America	34.4
South America	26.6
Global	20.2

Thermal conductivity

J75 Farouki (1986) Many parameters	$\kappa = K_e(\kappa_{sat} - \kappa_{dry}) + \kappa_{dry}$ $K_e = S_r$
MP81 **Independent on soil type** Validate on 3 soils	$\kappa = \begin{cases} \exp[-(PF + 2.7)] & PF <= 5.1 \\ 0.00041 & PF > 5.1 \end{cases}$
Cote & Konrad (2005) Based on J75,	$\kappa = K_e(\kappa_{sat} - \kappa_{dry}) + \kappa_{dry}$ $K_e = \frac{kS_r}{1 + (k-1)S_r}$
CLM3.0	$\lambda_i = \left\{ \begin{array}{ll} K_{e,i}\lambda_{sat,i} + (1 - K_{e,i})\lambda_{dry,i} & S_{r,i} > 1\times10^{-7} \\ \lambda_{dry,i} & S_{r,i} \le 1\times10^{-7} \end{array} \right\}$
Luo et al., 2009	k_s **use J75, dry soil thermal conductivity** k_{dry} Kersten number K_e Use Cote 2005

Soil water potential and hydraulic conductivity

	hydraulic conductivity	Soil water potential
Clapp and Hornberger (1978)	$k = k_{sat}\left(\theta_{liq}/\theta_{sat}\right)^{2b+3}$	$\psi = \psi_{sat}\left(\theta_{liq}/\theta_{sat}\right)^{-b}$
Zhao and Gray (1997)	$k = 10^{-E\theta_{ice}}\, k_{sat}\left(\frac{\theta_{liq}}{\theta_{sat}-\theta_{ice}}\right)^{2b+3}$ $\mathrm{E} = 7.0$	$\psi = \psi_{sat}\left(\frac{\theta_{liq}}{\theta_{sat}-\theta_{ice}}\right)^{-b}$
Kulik (1978) Koren (1999)	$k = 10^{-E\theta_{ice}}\, k_{sat}\left(\frac{\theta_{liq}}{\theta_{sat}}\right)^{2b+3}$ $E = \frac{5}{4}\left(K_{sat}-3\right)^2 + 6$	$\psi = \psi_{sat}\left(\frac{\theta_l}{\theta_{sat}}\right)^{-b}\left(1+c_k\theta_i\right)^2$
CLM3.5	$k = (1-F_{frz})\, k_{sat}\left(\frac{\theta}{\theta_{sat}}\right)^{2b+3}$	$\psi = \psi_{sat}\left(\frac{\theta}{\theta_{sat}}\right)^{-b}, \theta = \theta_{ice}+\theta_{liq}$
O'Neill et al. (1985)	$k_i = k_s\left(\frac{\theta_{sat}-\theta_{ice}}{\theta_{sat}}\right)^{9}\cdot\left(\frac{\theta_i}{\theta_{sat}}\right)^{2b+3}$	$F_{frz} = e^{-\alpha(1-\theta_i/\theta_s)} - e^{-\alpha}$ $\quad \alpha = 3.0$

Observed（black）and Simulated Snow Borderline （SCF=0.5）In Eurasian Continent

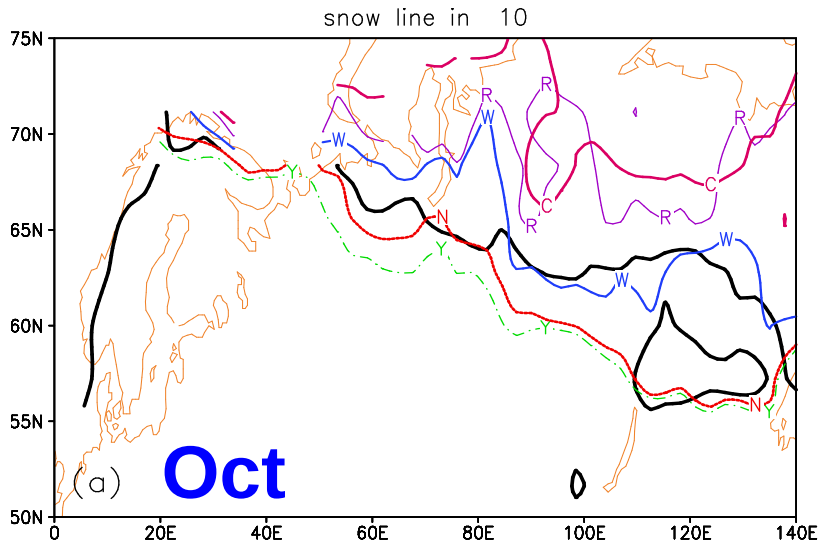

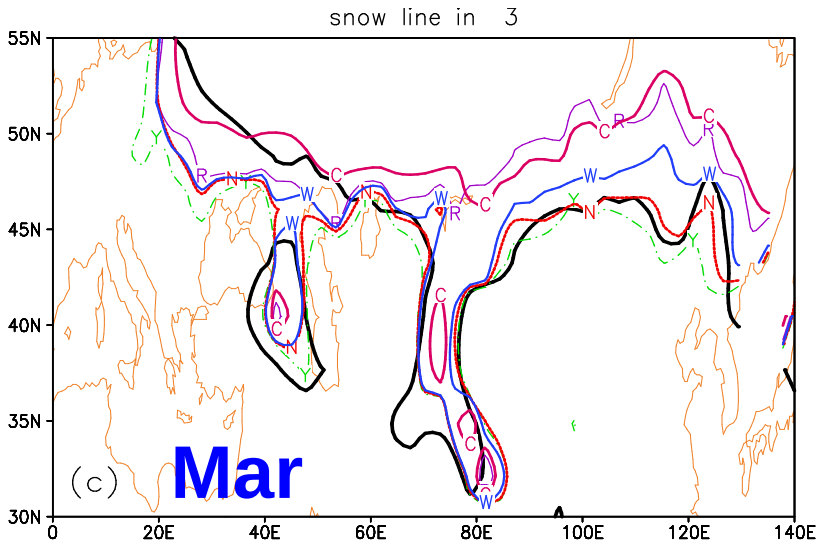

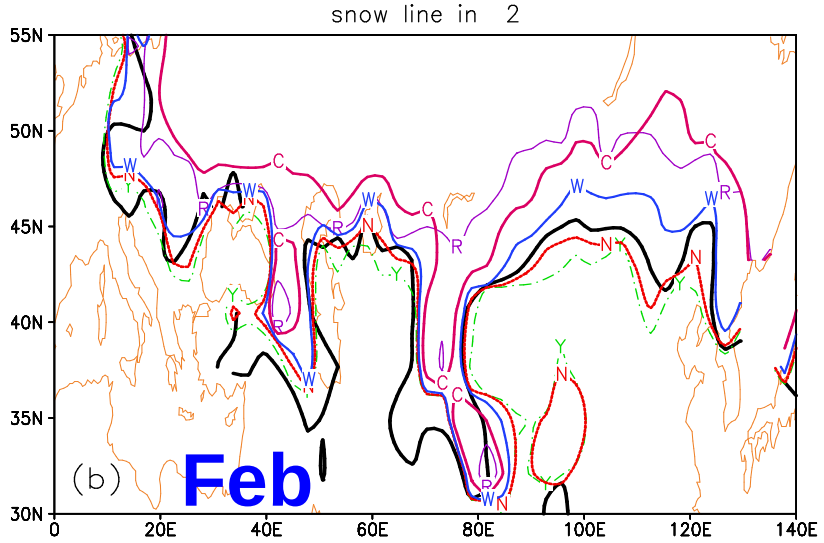

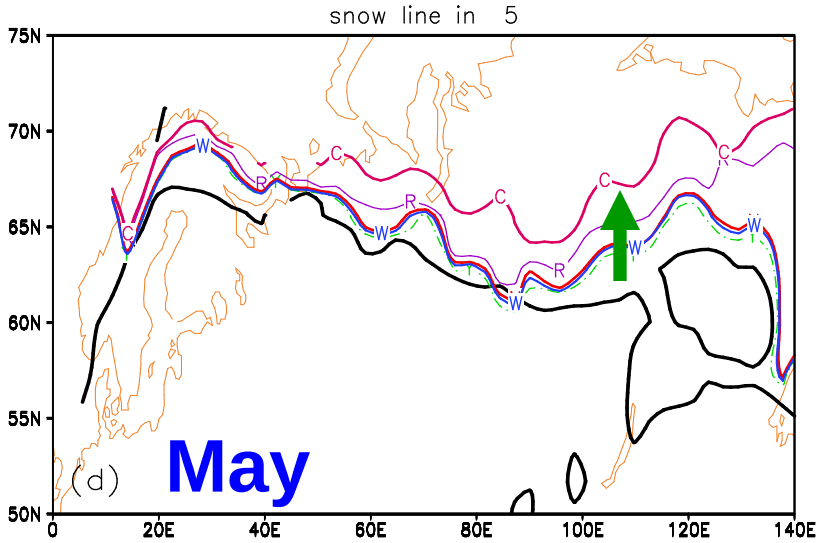

Observed（black）and Simulated Snow Borderline （SCF=0.5） In North American Continent

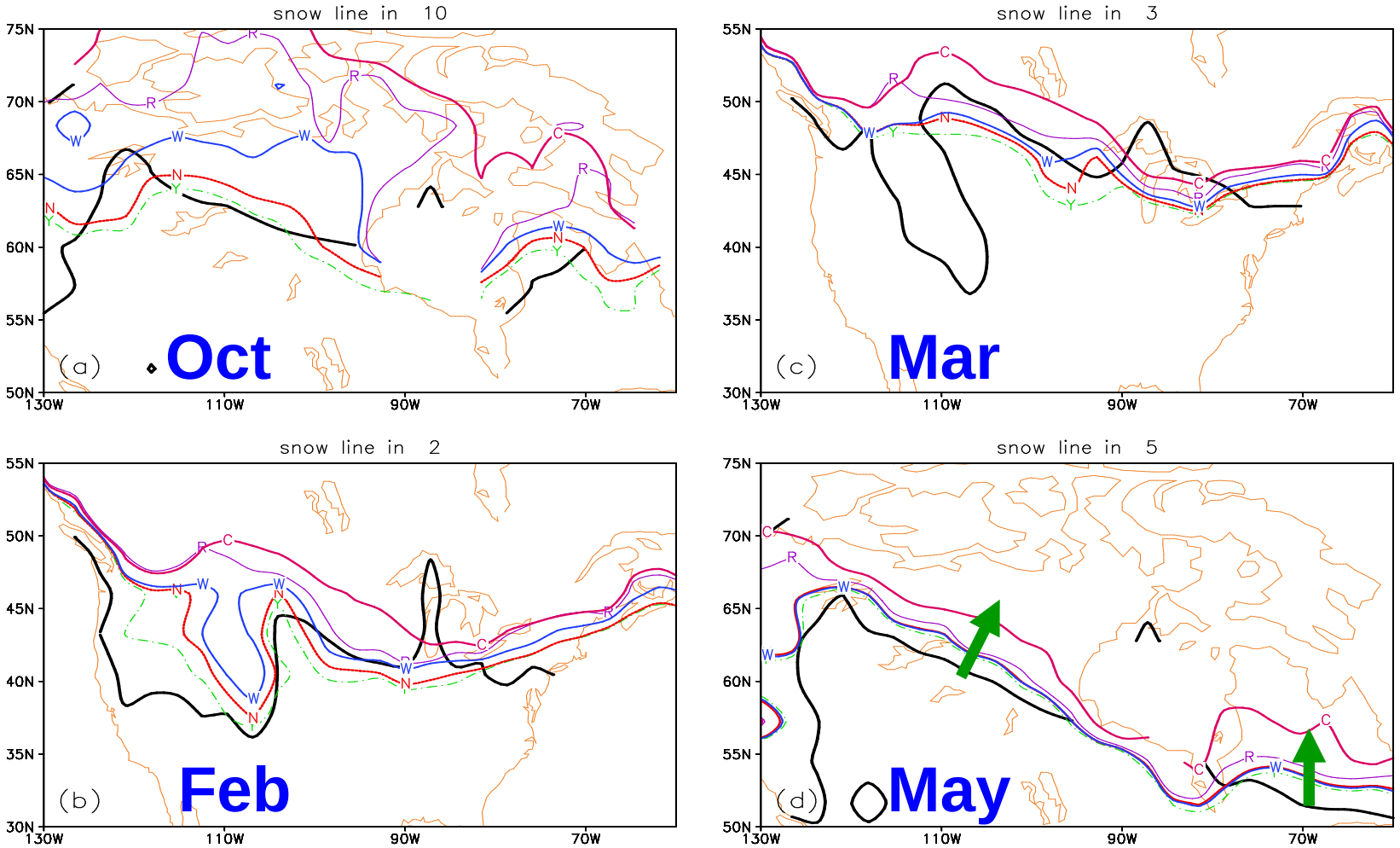

CLM3、Douville、Roesch schemes, northward drift of southern snow borderline in autumn and late spring